Manufactured Solutions for One-equation Turbulence Models in a Two-Dimensional Steady Wall-Bounded Incompressible Turbulent Flow

Eça L.
Instituto Superior Técnico (IST)

Hoekstra M.
Maritime Research Institute Netherlands (MARIN)

Hay A.
Ecole Polytechnique de Montréal (EPM)

Pelletier D.
Ecole Polytechnique de Montréal (EPM)

IST Report D72-36

EPM Report EMP-RT-2006-02

February 2006

Abstract

This report presents Manufactured Solutions for code and calculation verification of two-dimensional, steady, wall-bounded, incompressible, turbulent flows. The proposed solutions are specifically dedicated to one-equation models that solve a transport equations for a dependent variable that is directly related to the eddy-viscosity: the one-equation models of Spalart & Allmaras and Menter. The main flow variables are identical to the ones of an existing manufactured solution. The specified flow field satisfies mass conservation, but it requires additional source terms in the momentum equations.

The solutions obtained with the proposed manufactured solutions of the turbulence models dependent variable with a second-order accurate finite-difference method show that in these one-equation models it may not be easy to obtain the theoretical order of accuracy. Furthermore, the construction of the manufactured turbulence quantities as to be done carefully to avoid instabilities in the numerical solutions. The problem is model dependent: for the three manufactured solutions tested, the performance of the Spalart & Allmaras and Menter models is always different.

Contents

1 Introduction

Recently a Manufactured Solution (MS) has been proposed in [1] for code and calculation verification of two-dimensional, steady, wall-bounded, incompressible, turbulent flows. The MS is defined in a squared domain where the bottom boundary intends to mimic a wall in turbulent flow. The MS specifies the two velocity components, the pressure, the eddy-viscosity and the turbulence quantities required to obtain the desired eddy-viscosity field for six turbulence models:

1. The Spalart & Allmaras one-equation model, [2].
2. Menter's one-equation model, [3].
3. The standard $k - \epsilon$ two-equation model, [4].
4. Chien's low-Reynolds $k - \epsilon$ two-equation model, [5].
5. The turbulent/non-turbulent (TNT) $k - \omega$ two-equation model, [6].
6. Menter's baseline (BSL) $k - \omega$ two-equation model, [7].

The MS proposed in [1] includes manufactured functions for the eddy-viscosity and the turbulence kinetic energy. However, as discussed in [1], in the context of a MS the specification of the eddy-viscosity in the one-equation models is troublesome due to the behaviour of the damping functions included in the models. Therefore, for the Spalart & Allmaras and Menter one-equation models the MS specifies the dependent variable of the model instead of the eddy-viscosity.

Although the purpose of the MS is not to evaluate or compare turbulence models, one might feel tempted to compare the numerical performance obtained with different turbulence models. However, such comparisons may even be unfair. In the MS proposed in [1], the manufactured solutions for k, ϵ and ω are simpler than the manufactured eddy-viscosity, ν_t. Therefore, the one-equation models are "penalized" in such comparison. On the other hand, if a given model leads to an unexpected poor performance of the flow solver for a given MS, it is important to find the reasons for such behaviour.

The report [8] presents the results obtained with the finite-differences version of PARNASSOS, [9], for the calculation of the MS proposed in [1]. Three types of exercises have been performed:

1. Solve numerically the turbulence model transport equation(s) using the manufactured velocity field.

2. Calculate the velocity and pressure field using the manufactured eddy-viscosity.

3. Compute the complete flow field.

The first and third exercises were performed for the six turbulence models considered in [1].

The results presented in [8] show that it is relatively straightforward to attain the asymptotic range in the solution of the continuity and momentum equations with the manufactured eddy-viscosity field (exercice 2 of the list above). In exercise 3, however, the solution of the turbulence quantities transport equations may have a significant effect on the observed order of accuracy of the main flow quantities for the same grid density. With the four two-equation models tested, these observed orders of accuracy are not as regular as the ones obtained with the manufactured ν_t, but they are still close to the theoretical order of the method. However, the results obtained with the one-equation turbulence models exhibit an irregular behaviour of the observed order of accuracy, p, which in the case of the Spalart & Allmaras model is clearly below the theoretical order of the method. With this turbulence model in exercise 1 (the calculation of the eddy-viscosity with the manufactured velocity field) the results revealed that the near-bottom solution of the dependent variable, $\tilde{\nu}$, converges very slowly. In the original MS, [1], $\tilde{\nu}$ in the "near-wall" region varies with the fourth power of the distance to the bottom. On the other hand, with an alternative MS that depends on the second power of the distance to the bottom, the convergence properties (error level and p) obtained with the same model is substantially improved. Therefore, this report presents two alternative MS's for the one-equation models.

As a first check of the dependence of the flow solution on the MS proposed for $\tilde{\nu}$, we have compared the results obtained with the three alternative MS's (original MS plus 2 MS's proposed in this report) in the calculation of the turbulence models transport equation with a manufactured velocity field, i.e. we have assumed a frozen velocity field in the flow solution. The results presented in [8] suggest that this type of exercise indicates the existence of any numerical problems for the complete flow solution.

The report is organized in the following way: the manufactured solutions are presented in section 2, which for the sake of completeness includes also the description of the previous MS, [1]. The two one-equation models are briefly described in section 3. The calculations of the three MS's with the finite-differences version of PARNASSOS are presented and discussed in section 4. The conclusions of this report are summarized in section 5. The appendix A presents tables

with the observed order of accuracy of the turbulence quantities determined for different groups of grids and the appendix B presents the list of FORTRAN functions with all the flow quantities and source terms of the MS.

2 Manufactured Solutions

2.1 General

A Manufactured Solution (MS) created for a steady, incompressible, near-wall turbulent flow is presented in [1]. In this report, we present two alternative solutions for the dependent variable of the one-equation turbulence models of Spalart & Allmaras and Menter. The main variables of the proposed flow field remain unchanged. Nevertheless, for the sake of completeness, we present all the manufactured variables required for a flow calculation with the one-equation models.

The computational domain is a square of side 0.5L with $0.5L \leq X \leq L$ and $0 \leq Y \leq 0.5L$ and the proposed Reynolds number, Rn, is 10^6.

$$Rn = \frac{U_1 L}{\nu} \ , \tag{1}$$

where U_1 is the reference velocity, L the reference length and ν the kinematic viscosity. In non-dimensional variables, (x, y), the computational domain is given by $0.5 \leq x \leq 1$ and $0 \leq y \leq 0.5$, where x stands for the horizontal direction and y for the vertical direction.

2.2 Main flow variables

In the definition of the velocity components and pressure coefficient we will use the following quantity:

$$\eta = \frac{\sigma y}{x} \ , \tag{2}$$

where is $\sigma = 4$.

2.2.1 Horizontal velocity component, u_x

The velocity component in the x direction, u, is given by

$$u_x = \mathrm{erf}(\eta) \ . \tag{3}$$

Equation (3) does not reproduce accurately the features of a near-wall turbulent flow. Nevertheless, the main goal of including a no-slip condition at the bottom is satisfied.

2.2.2 Vertical velocity component, u_y

The velocity component in the y direction, u_y, is constructed to satisfy mass conservation in an incompressible flow, i.e. a divergence free velocity field.

$$u_y = \frac{1}{\sigma\sqrt{\pi}}\left(1 - e^{-\eta^2}\right) \ . \tag{4}$$

2.2.3 Pressure, P

The pressure is given by

$$C_p = \frac{P}{\rho(U_1)^2} = 0.5\ln\left(2x - x^2 + 0.25\right)\ln\left(4y^3 - 3y^2 + 1.25\right) \tag{5}$$

2.3 Turbulence quantities of the one-equation models

In this section we will designate the dependent variable of the one-equation turbulence models of Spalart & Allmaras and Menter by $\tilde{\nu}$. As discussed in [1], a MS in the one-equation models should define the dependent variable of the model instead of the eddy-viscosity, ν_t. The manufactured ν_t will be a consequence of the manufactured $\tilde{\nu}$ and of the damping functions of the model.

2.3.1 Eddy-viscosity, ν_t

In the Spalart & Allmaras model, [2], ν_t is given by

$$\nu_t = \tilde{\nu} f_{v1} \tag{6}$$

with

$$f_{v1} = \frac{\chi^3}{\chi^3 + c_{v1}^3} \tag{7}$$

and

$$\begin{aligned} \chi &= \frac{\tilde{\nu}}{\nu} , \\ c_{v1} &= 7.1 . \end{aligned} \tag{8}$$

For the Menter model, [3], the eddy-viscosity is obtained from

$$\nu_t = D_2 \tilde{\nu} , \tag{9}$$

where

$$D_2 = 1 - e^{-\left(\frac{\tilde{\nu}}{A^+ \kappa \nu}\right)^2} \tag{10}$$

and

$$\begin{aligned} A^+ &= 13 , \\ \kappa &= 0.41 . \end{aligned} \tag{11}$$

2.3.2 Dependent variable of the turbulence models, $\tilde{\nu}$

In the MS proposed in [1], $\tilde{\nu}$ is given by

$$\tilde{\nu} = 0.25 \nu_{max} \eta_\nu^4 e^{2-\eta_\nu^2} , \tag{12}$$

where

$$\eta_\nu = \frac{\sigma_\nu y}{x} , \tag{13}$$

$\sigma_\nu = 2.5\sigma$ and ν_{max} is $10^3 \nu$.

Close to the bottom, ν_t varies with y^4 as in a near-wall turbulent flow. However, in the MS this behaviour will be partially propagated along all the vertical direction. We will refer to this solution as MS4.

To avoid the numerical difficulties imposed by the y^4 dependence of $\tilde{\nu}$ in MS4, an alternative manufactured $\tilde{\nu}$ is proposed. In this MS, $\tilde{\nu}$ is given by

$$\tilde{\nu} = \nu_{max} \eta_\nu^2 e^{1-\eta_\nu^2} , \tag{14}$$

Equation (14) is similar to the one of the original MS, (12), but in this case $\tilde{\nu}$ depends only on the second power of the distance to the bottom, y^2. We will designate this case by MS2.

A third possibility was also considered for the definition of $\tilde{\nu}$, MS1. The proposed function varies linearly with y in the near-bottom region and present the same exponential decays of the other two MS's.

$$\tilde{\nu} = \nu_{max}\sqrt{2}\eta_\nu e^{0.5-\eta_\nu^2} \ . \tag{15}$$

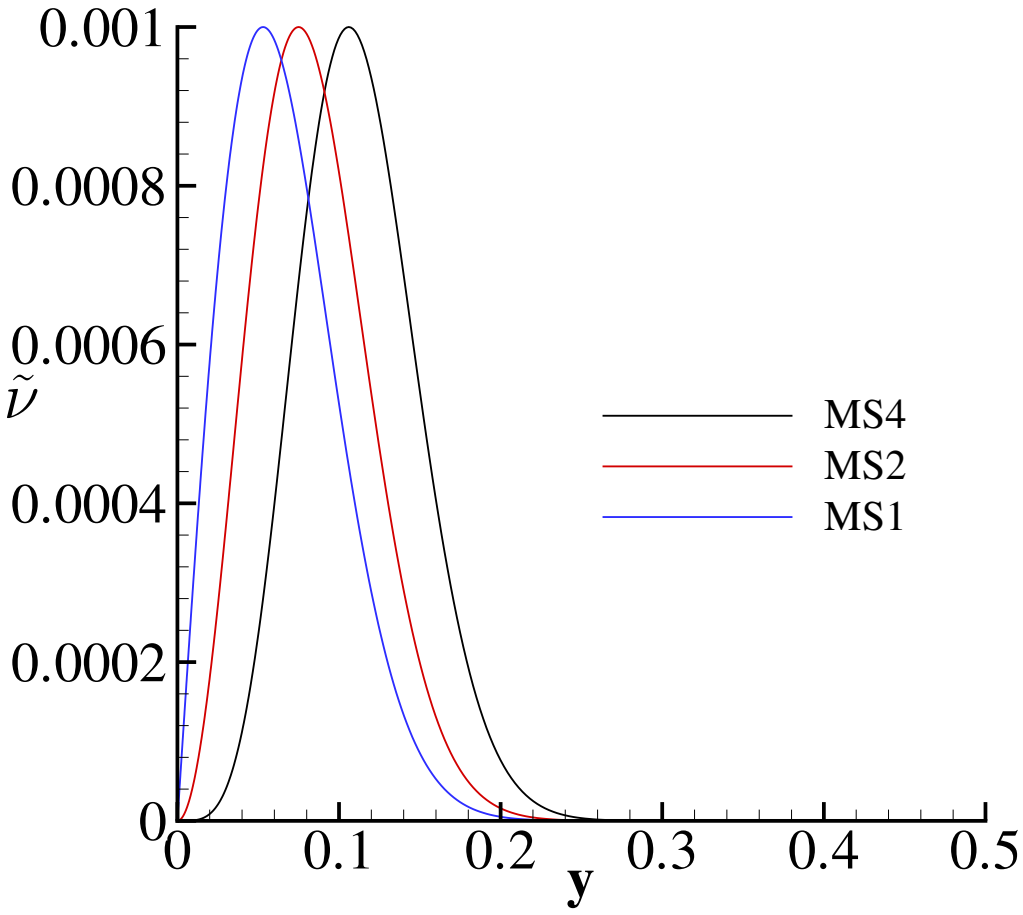

Figure 1: Manufactured profiles of $\tilde{\nu}$ at x=0.75.

Figure 1 presents the three manufactured profiles of $\tilde{\nu}$ at $x = 0.75$. The maximum of $\tilde{\nu}$ is identical in the three solutions but it occurs at three different locations: $\eta_\nu = \sqrt{2}$ for the MS4, $\eta_\nu = 1$ for the MS2 and $\eta_\nu = \frac{\sqrt{2}}{2}$ for the MS1. A detailed view of the near-bottom $\tilde{\nu}$ profiles is presented in figure 2.

The calculation of the source terms of the turbulence models transport equations of the MS2 and MS1 requires the first and second derivatives of $\tilde{\nu}$ with

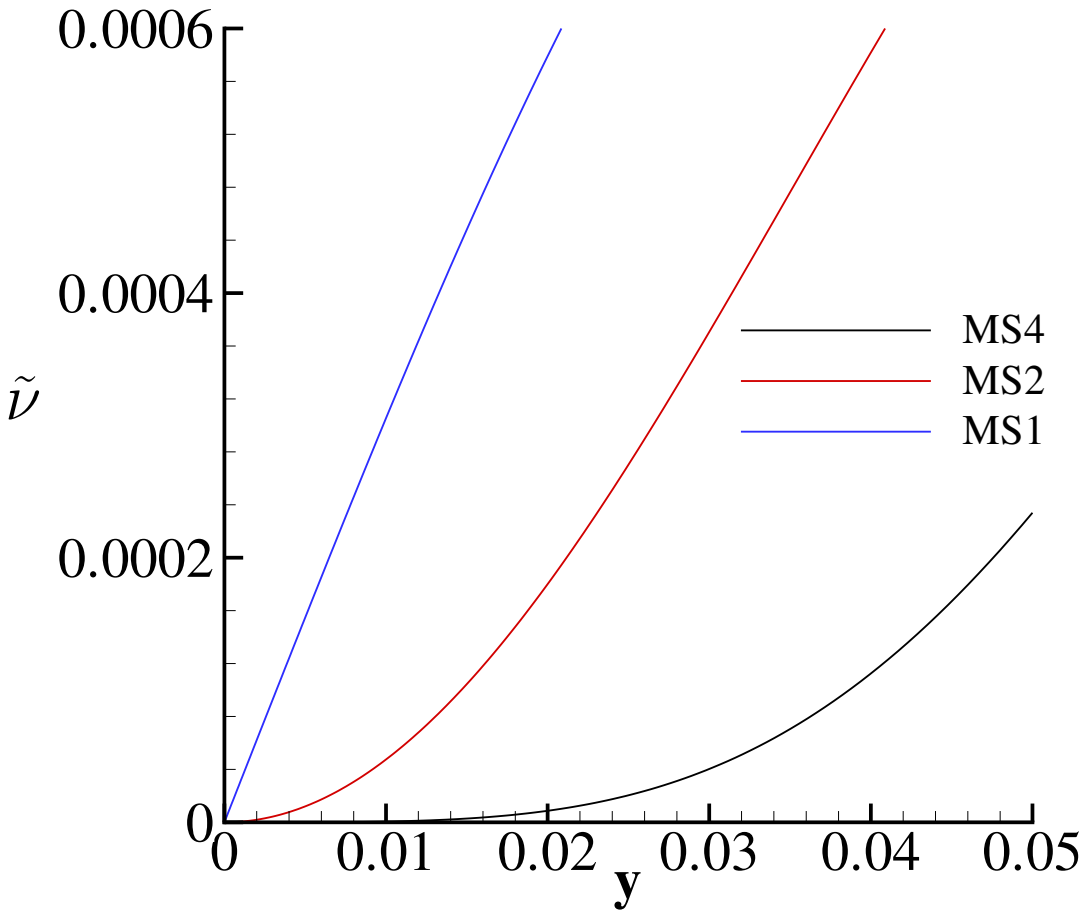

Figure 2: Manufactured profiles of $\tilde{\nu}$ in the near-bottom region at x=0.75.

respect to x and y, which are given by:

- MS2 definition of $\tilde{\nu}$, equation (14)

  - First derivatives

$$\begin{aligned} \frac{\partial \tilde{\nu}}{\partial x} &= 2\frac{\tilde{\nu}}{x}\left(\eta_\nu^2 - 1\right) \\ \frac{\partial \tilde{\nu}}{\partial y} &= 2\frac{\tilde{\nu}}{y}\left(1 - \eta_\nu^2\right) \end{aligned} \tag{16}$$

– Second derivatives

$$\begin{aligned} \frac{\partial^2 \tilde{\nu}}{\partial x^2} &= 2\frac{\tilde{\nu}}{x^2}\left(2\eta_\nu^4 - 7\eta_\nu^2 + 3\right) \\ \frac{\partial^2 \tilde{\nu}}{\partial y^2} &= 2\frac{\tilde{\nu}}{y^2}\left(2\eta_\nu^4 - 5\eta_\nu^2 + 1\right) \ . \end{aligned} \tag{17}$$

- MS1 definition of $\tilde{\nu}$, equation (15)

  – First derivatives

$$\begin{aligned} \frac{\partial \tilde{\nu}}{\partial x} &= \frac{\tilde{\nu}}{x}\left(2\eta_\nu^2 - 1\right) \\ \frac{\partial \tilde{\nu}}{\partial y} &= \frac{\tilde{\nu}}{y}\left(1 - 2\eta_\nu^2\right) \end{aligned} \tag{18}$$

  – Second derivatives

$$\begin{aligned} \frac{\partial^2 \tilde{\nu}}{\partial x^2} &= 2\frac{\tilde{\nu}}{x^2}\left(2\eta_\nu^4 - 5\eta_\nu^2 + 1\right) \\ \frac{\partial^2 \tilde{\nu}}{\partial y^2} &= 2\frac{\tilde{\nu}}{y^2}\left(2\eta_\nu^4 - 3\eta_\nu^2\right) \ . \end{aligned} \tag{19}$$

3 One-equation Turbulence Models

Two one-equation turbulence models have been considered for the specification of the Manufactured Solutions: Spalart & Allmaras, [2], and Menter, [3], models. This section includes a brief description of both models.

In the context of the Method of the Manufactured Solutions, a source term has to be included in the turbulence quantities transport equation. The definition of this source term is also presented below.

3.1 Spalart & Allmaras

The Spalart & Allmaras model proposed in [2] solves the following transport equation:

$$u\frac{\partial \tilde{\nu}}{\partial x} + v\frac{\partial \tilde{\nu}}{\partial y} = c_{b1}\tilde{S}\tilde{\nu} + \frac{1}{\sigma_s}\left[\nabla\cdot\left((\nu+\tilde{\nu})\nabla\tilde{\nu}\right) + c_{b2}\left(\nabla\tilde{\nu}\cdot\nabla\tilde{\nu}\right)\right] - c_{w1}f_w\left[\frac{\tilde{\nu}}{d}\right]^2 , \tag{20}$$

where

$$\begin{aligned}
S_\Omega &= \left|\frac{\partial u}{\partial y} - \frac{\partial v}{\partial x}\right| \\
\tilde{S} &= S_\Omega + \frac{\tilde{\nu}}{\kappa^2 d^2} f_{v2} \\
d &= y \\
f_w &= g\left[\frac{1+c_{w3}^6}{g^6+c_{w3}^6}\right]^{\frac{1}{6}} \\
f_{v2} &= 1 - \frac{\chi}{1+\chi f_{v1}} \\
g &= r + c_{w2}\left(r^6 - r\right) \\
r &= \frac{\tilde{\nu}}{\tilde{S}\kappa^2 d^2} \\
\chi &= \frac{\tilde{\nu}}{\nu} \\
f_{v1} &= \frac{\chi^3}{\chi^3 + c_{v1}^3}
\end{aligned} \tag{21}$$

The eddy-viscosity is obtained from

$$\nu_t = \tilde{\nu} f_{v1} \tag{22}$$

The model constants are :

$$\begin{array}{lll}
\kappa = 0.41\ , & c_{b1} = 0.1355\ , & c_{b2} = 0.622 \\
c_{w1} = 3.2391\ , & c_{w2} = 0.3\ , & c_{w3} = 2. \\
c_{v1} = 7.1\ , & \sigma_s = \frac{2}{3}\ . &
\end{array}$$

The MS is obtained specifying $\tilde{\nu}$ from equations (12), (14) or (15).

The source function to be added to the right-hand side of the transport equation of $\tilde{\nu}$, equation (20), is given by:

$$f_{spal} = T_{cs} + T_{ds} + T_{ps} + T_{dis} \tag{23}$$

where

$$\begin{aligned} T_{cs} &= u\frac{\partial\tilde{\nu}}{\partial x} + v\frac{\partial\tilde{\nu}}{\partial y} \\ T_{ds} &= -\frac{1}{\sigma_s}\left[(\nu+\tilde{\nu})\left(\frac{\partial^2\tilde{\nu}}{\partial x^2}+\frac{\partial^2\tilde{\nu}}{\partial y^2}\right) + (1+c_{b2})\left(\left(\frac{\partial\tilde{\nu}}{\partial x}\right)^2+\left(\frac{\partial\tilde{\nu}}{\partial y}\right)^2\right)\right] \\ T_{ps} &= -c_{b1}\tilde{S}\tilde{\nu} \\ T_{dis} &= c_{w1}f_w\left[\frac{\tilde{\nu}}{d}\right]^2 \end{aligned} \tag{24}$$

3.2 Menter

The one-equation model proposed by Menter in [3] solves the following transport equation :

$$u\frac{\partial\tilde{\nu}_t}{\partial x} + v\frac{\partial\tilde{\nu}_t}{\partial y} = c_1 D_1\tilde{\nu}_t\sqrt{S} + \nabla\cdot\left((\nu+\frac{\tilde{\nu}_t}{\sigma})\nabla\tilde{\nu}_t\right) - c_2 E_{1e}. \tag{25}$$

The eddy-viscosity is given by

$$\nu_t = D_2\tilde{\nu}_t \tag{26}$$

and

$$\begin{aligned} S &= 2\left(\left(\frac{\partial u}{\partial x}\right)^2+\left(\frac{\partial v}{\partial y}\right)^2\right)+\left(\frac{\partial u}{\partial y}+\frac{\partial v}{\partial x}\right)^2 \\ D_1 &= \frac{\nu_t+\nu}{\tilde{\nu}_t+\nu} \\ E_{1e} &= c_3 E_{BB}\tanh\left(\frac{E_{k-\epsilon}}{c_3 E_{BB}}\right) \\ D_2 &= 1-e^{-\left(\frac{\tilde{\nu}_t}{A^+\kappa\nu}\right)^2} \\ E_{k-\epsilon} &= \tilde{\nu}_t^2\left(\frac{\nabla\sqrt{S}\cdot\nabla\sqrt{S}}{S}\right) \\ E_{BB} &= \nabla\tilde{\nu}_t\cdot\nabla\tilde{\nu}_t \end{aligned} \tag{27}$$

The model constants are :

$$\begin{array}{lll} c_1 = 0.144\ , & c_2 = 1.862\ , & c_3 = 7 \\ \kappa = 0.41\ , & \sigma = 1\ , & A^+ = 13\ . \end{array}$$

As for the Spalart & Allmaras turbulence model, $\tilde{\nu}_t$ is defined by equations (12), (14) or (15).

The source function to be added to the right-hand side of the transport equation of $\tilde{\nu}_t$, equation (25), is given by:

$$f_{mnt} = T_{cm} + T_{dm} + T_{pm} + T_{dim} \tag{28}$$

where

$$\begin{aligned}
T_{cm} &= u\frac{\partial \tilde{\nu}_t}{\partial x} + v\frac{\partial \tilde{\nu}_t}{\partial y} \\
T_{dm} &= -\left[\left(\nu + \frac{\tilde{\nu}_t}{\sigma}\right)\left(\frac{\partial^2 \tilde{\nu}_t}{\partial x^2} + \frac{\partial^2 \tilde{\nu}_t}{\partial y^2}\right) + \frac{1}{\sigma}\left(\left(\frac{\partial \tilde{\nu}_t}{\partial x}\right)^2 + \left(\frac{\partial \tilde{\nu}_t}{\partial y}\right)^2\right)\right] \\
T_{pm} &= -c_1 D_1 \sqrt{S}\tilde{\nu}_t \\
T_{dim} &= c_2 E_{1e}
\end{aligned} \tag{29}$$

4 Results of the Calculation of the Manufactured Solutions

4.1 Flow Solver

All the calculations were performed with the 2-D finite-difference version of PARNASSOS, [9], which solves the steady, incompressible, Reynolds-averaged Navier Stokes equations using eddy-viscosity turbulence models. The main properties of the flow solver are:

- The continuity and momentum equations are written in Contravariant form and the momentum balance is computed along the directions of the curvilinear coordinate system.
- A fully-collocated arrangement is adopted with the unknowns and the discretization centered at the grid nodes.
- Newton linearization is applied to the convective terms.
- Second-order schemes are applied in the discretization of diffusion and all the coordinate derivatives included in the metric coefficients.

- Velocity derivatives in the continuity equation and the pressure gradient are discretized with third-order schemes using a fixed bias.
- Third-order upwind discretization is applied to the convective terms of the momentum equations.
- The linear system of equations formed by the discretized continuity and momentum equations is solved simultaneously with GMRES, [10], using a coupled ILU preconditioning.
- Under-relaxation is applied with a quasi time-derivative term.
- The convective terms of the transport equations of the turbulence quantities are discretized with third-order upwind schemes.
- The linearization procedure of the production and dissipation terms of the turbulence quantities transport equations follows the standard approach, i.e. production is added to the right-hand side and dissipation to the main-diagonal.
- The solution of the turbulence quantities transport equations is uncoupled from solving the continuity and momentum equations.

4.2 Grid Sets

In the present report we have adopted the sets used in [8], i.e. Cartesian grids using three types of grid node distributions:

1. Equally-spaced grids in the x and y directions, Eq.
2. Equally-spaced grids in the x direction and clustered grid nodes close to the bottom boundary using a one-sided stretching function, [11]. Stretching parameter 0.05, ST1.
3. Equally-spaced grids in the x direction and clustered grid nodes close to the bottom boundary using a one-sided stretching function, [11]. Stretching parameter 0.005, ST2.

The three grid sets include 16 geometrically similar grids covering a grid refinement ratio of 4. The finest grid includes 401×401 grid nodes and the coarsest grid 101×101. For each set, there are 19×19 physical locations which always

	$NX \times NY$	Eq.	ST1	ST2		$NX \times NY$	Eq.	ST1	ST2
1	401×401	37.6	1.89	0.19	9	241×241	62.6	3.17	0.32
2	381×381	39.5	1.99	0.20	10	221×221	68.3	3.46	0.35
3	361×361	41.7	2.10	0.21	11	201×201	75.1	3.81	0.38
4	341×341	44.2	2.23	0.23	12	181×181	83.5	4.24	0.43
5	321×321	46.9	2.37	0.24	13	161×161	93.9	4.77	0.48
6	301×301	50.1	2.53	0.25	14	141×141	107.	5.47	0.55
7	281×281	53.7	2.71	0.27	15	121×121	125.	6.40	0.65
8	261×261	57.8	2.92	0.29	16	101×101	150.	7.72	0.78

Table 1: y_2^+ maximum for the 16 grids of the three grid sets.

coincide with grid nodes. Obviously, these locations are not the same for the three sets. However, this will allow the determination of the convergence properties of local flow quantities without requiring any sort of interpolation.

Although in the proposed MS the concept of y^+ looses its physical meaning, table 1 presents the maximum value of y^+ at the first grid node away from the bottom, y_2^+.

$$y^+ = \frac{y\sqrt{\nu\left(\dfrac{\partial u_x}{\partial y}\right)_{y=0}}}{\nu}$$

where u_x is the (horizontal) velocity component in the x direction. Obviously, this table is valid for the three MS's, because the manufactured velocity field is always the same. Table 1 also includes the number that designates each grid of the three sets in the tables of appendix A.

4.3 Monitoring the Error

We have assumed the usual, [12], representation of the error of any flow quantity, ϕ, using a power series expansion where we have neglected all high-order terms.

$$e(\phi) = \phi - \phi_{ms} \simeq \alpha h_i^p \ , \tag{30}$$

where the subscript $_{ms}$ identifies the manufactured solution, α is a constant, h_i is the typical cell size and p is the order of accuracy.

For the present grids,

$$h_i = \frac{1}{NX} = \frac{1}{NY} \ .$$

NX and NY stand for the number of nodes in the x and y directions.

We have adopted two types of quantities to monitor the error of the numerical solution:

1. Global quantities which represent average values over the complete grid.

2. Local quantities at selected locations.

For each turbulence quantity, we have computed the Root Mean Square (RMS) of the error of the numerical solution, which is given by:

$$RMS(e(\phi)) = \sqrt{\sum_{i=2}^{NX-1} \sum_{j=2}^{NY-1} \frac{(\phi(j,i) - \phi(j,i)_{ms})^2}{(NX-2)(NY-2)}} \tag{31}$$

where i is the index of the node in the x direction and j is the index of the node in the y direction.

There is no guarantee that the convergence of the flow field is uniform in all the computational domain (i.e. p constant for all the field) and so we have also analyzed the error at 8 fixed locations of the three grid sets. At this stage, we have avoided the use of interpolation in the post-processing and so the 8 locations are not common to the three grid sets. The i and j indexes are given in table 2, which includes also the x and y coordinates of the selected locations.

In the results presented in the remainder of this section, the observed order of accuracy, p, and the constant α are determined with a least squares root approach, [13]. The fits plotted in the figures are obtained with the data of the 11 finest grids of each set, i.e. the grids with at least 201×201 grid nodes, covering a grid refinement ratio of 2. However, we have also checked the dependence of the observed order of accuracy on the selected grids. The observed order of accuracy is estimated for different groups of grids, which must present a grid refinement ratio between the finest and coarsest grid, $r_{i1} = h_i/h_1$, of at least 1.3. This is an important check, because it indicates if the data obtained in the finest grids are in the so-called 'asymptotic range'. These results are presented in the tables of appendix A.

	All Sets			Eq	ST1	ST2
	i	j	x	$y \times 10^{+2}$	$y \times 10^{+3}$	$y \times 10^{+4}$
P1	$1 + 2\Delta_x$	$1 + \Delta_y$	0.55	2.50	1.43	1.54
P2	$1 + 4\Delta_x$	$1 + 2\Delta_y$	0.60	5.00	3.30	3.85
P3	$1 + 6\Delta_x$	$1 + 3\Delta_y$	0.65	7.50	5.73	7.31
P4	$1 + 8\Delta_x$	$1 + 4\Delta_y$	0.70	10.0	8.89	12.5
P5	$1 + 10\Delta_x$	$1 + 5\Delta_y$	0.75	12.5	13.0	20.2
P6	$1 + 12\Delta_x$	$1 + 6\Delta_y$	0.80	15.0	18.3	31.8
P7	$1 + 14\Delta_x$	$1 + 7\Delta_y$	0.85	17.5	25.2	49.1
P8	$1 + 16\Delta_x$	$1 + 8\Delta_y$	0.90	20.0	34.0	74.8
	$\Delta_x = (NX - 1)/20$			$\Delta_y = (NY - 1)/20$		

Table 2: Coordinates of the 8 selected locations to monitor the convergence of the numerical solution with the grid refinement.

4.4 Calculation of the eddy-viscosity field with the manufactured velocity field

The influence of the turbulence model on the convergence properties of the flow solution has been checked by the calculation of the eddy-viscosity field using the manufactured velocity field. It should be mentioned that any flow quantities involving the velocity derivatives, like the vorticity magnitude or the strain rate, have been computed numerically.

For each of the manufactured $\tilde{\nu}$ fields, MS4, MS2 and MS1, three grid refinement studies have been performed with the manufactured velocity field for the two one-equation turbulence models. All calculations have been converged to machine accuracy using a 15 digits precision.

4.4.1 Boundary Conditions

In these calculations, Dirichlet boundary conditions were applied at the four boundaries of the computational domain for all the turbulence quantities.

In PARNASSOS, there are two-layers of virtual grid nodes at each boundary of the computational domain. These virtual grid nodes guarantee that the stencil of the third-order schemes can be kept in the vicinity of the boundaries of the domain. In the present calculations, we have filled-in these virtual layers using quadratic

extrapolation based on the boundary node and its two closest neighbours, i.e. the manufactured solution is only specified at the boundaries of the computational domain.

4.4.2 Spalart & Allmaras one-equation model

Surprisingly, the numerical convergence of the Spalart & Allmaras model with the MS1 is troublesome. The problems increase with the reduction of the near-bottom grid line spacing. Although it is possible to obtain a converged solution for all the grids of sets Eq, ST1 and ST2, an extremely small (below 0.01) under-relaxation parameter is required for the ST1 and ST2 grids to converge the solutions to machine accuracy. The problems are originated by the non-linear production and dissipation terms of the $\tilde{\nu}$ transport equation. Therefore, we have performed the calculations for the ST1 and ST2 sets with the production and dissipation terms evaluated directly from the manufactured solution rather than using their numerical discretizations. These two cases will be designated by ST1$_{ms}$ and ST2$_{ms}$.

The convergence of the RMS of the error of $\tilde{\nu}$ as a function of the grid refinement ratio is illustrated in figure 3 for the MS4, MS2 and MS1 in the three grid sets, Eq, ST1 and ST2. The observed order of accuracy at the 8 selected locations of each grid set is given in tables 3 to 5 of appendix A.

There are several interesting features in the data presented in figure 3 and tables 3 to 5:

- For all the grid sets and for a given number of grid nodes, the smallest error is always obtained for the MS1 and the largest error for the MS4. The MS2 error level is clearly closer to the MS1 data than to the MS4 results.

- The influence of the grid line spacing on the error level is not the same for the three MS's. In the MS4, with the same number of grid nodes, the lowest errors are obtained for the ST1 set and the largest errors for the ST2 set. On the other hand, the MS2 and MS1 also exhibit the lowest errors for the ST1 set, but the largest errors are obtained with the equally-spaced grids, set Eq.

- There is consistency between the observed order of accuracy, p, of the RMS of the error of $\tilde{\nu}$ for the same MS in the three grid sets. However, the value p is not the same for the three MS's: p is 1 for the MS4, and p is equal to the theoretical order of the numerical method, $p = 2.0$, for the MS2 and MS1.

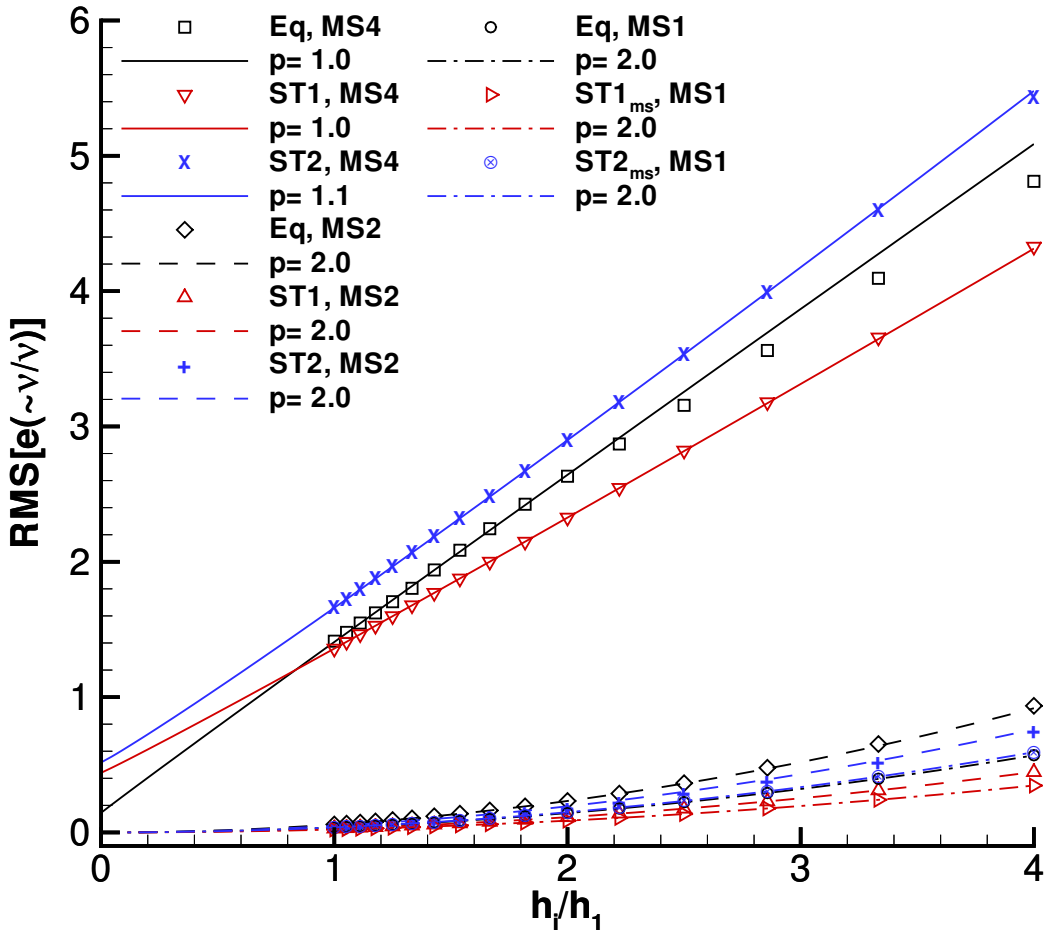

Figure 3: Convergence of the RMS of the error of $\tilde{\nu}$ with the grid refinement in the grid sets Eq, ST1 and ST2. Spalart & Allmaras one-equation model.

However, one must not forget that the MS1 solution was computed with the manufactured dissipation and production terms for the ST1 and ST2 sets.

- Most of the 8 locations selected in each grid set exhibit an observed order of accuracy which is in the "asymptotic range", i.e. it does not change with the number of grids selected. However, there are a few exceptions. The RMS of the error also exhibits a well established observed order of accuracy with a single exception, the MS4 in the Eq set. Values of p too large or close to 0 are a consequence of nearly grid independent solutions that lead to an ill-conditioned problem for the determination of p.

- The observed order of accuracy of $\tilde{\nu}$ is not independent of the location selected. Although the consistency of p at the 8 selected locations depends on the MS and grid set selected, it is clear that the observed order of accuracy of the RMS of the error may not be representative of the convergence properties at different physical locations of the computational domain.

The results presented above show different convergence properties for the three alternative MS's. Therefore, we have investigated the convergence of the several terms of the $\tilde{\nu}$ transport equation, [2]:

1. Convection, C_ν.
$$u\frac{\partial\tilde{\nu}}{\partial x} + v\frac{\partial\tilde{\nu}}{\partial y}$$
2. Diffusion, Df_ν.
$$-\frac{1}{\sigma_s}\left[\nabla\cdot\left((\nu+\tilde{\nu})\nabla\tilde{\nu}\right) + c_{b2}\left(\nabla\tilde{\nu}\cdot\nabla\tilde{\nu}\right)\right]$$
3. Production, P_ν.
$$-c_{b1}\left(S_\Omega + \frac{\tilde{\nu}}{\kappa^2 d^2}f_{v2}\right)\tilde{\nu}$$
4. Dissipation, Ds_ν.
$$c_{w1}f_w\left[\frac{\tilde{\nu}}{d}\right]^2$$

Although the MS1 calculations were performed with the manufactured production and dissipation terms for the ST1 and ST2 sets, we have computed the error of these terms in the converged solution. These results are fundamental to understand the problems obtained for this particular MS.

The RMS of the error of the four terms of the $\tilde{\nu}$ transport equation are plotted in figure 4 as a function of the typical cell size for the ST1 set. Tables 4 to 7 of the appendix A present the observed order of accuracy of C_ν, Df_ν, P_ν and Ds_ν at the 8 selected locations of the set ST1. The values of p for the RMS are also included in the tables 4 to 7. The results plotted in figure 4 for the dissipation term of the MS1 solution are divided by 10.

The data presented in figure 4 and tables 4 to 7 show the origin of the unexpected results obtained for the MS1 and MS4:

- MS1 case

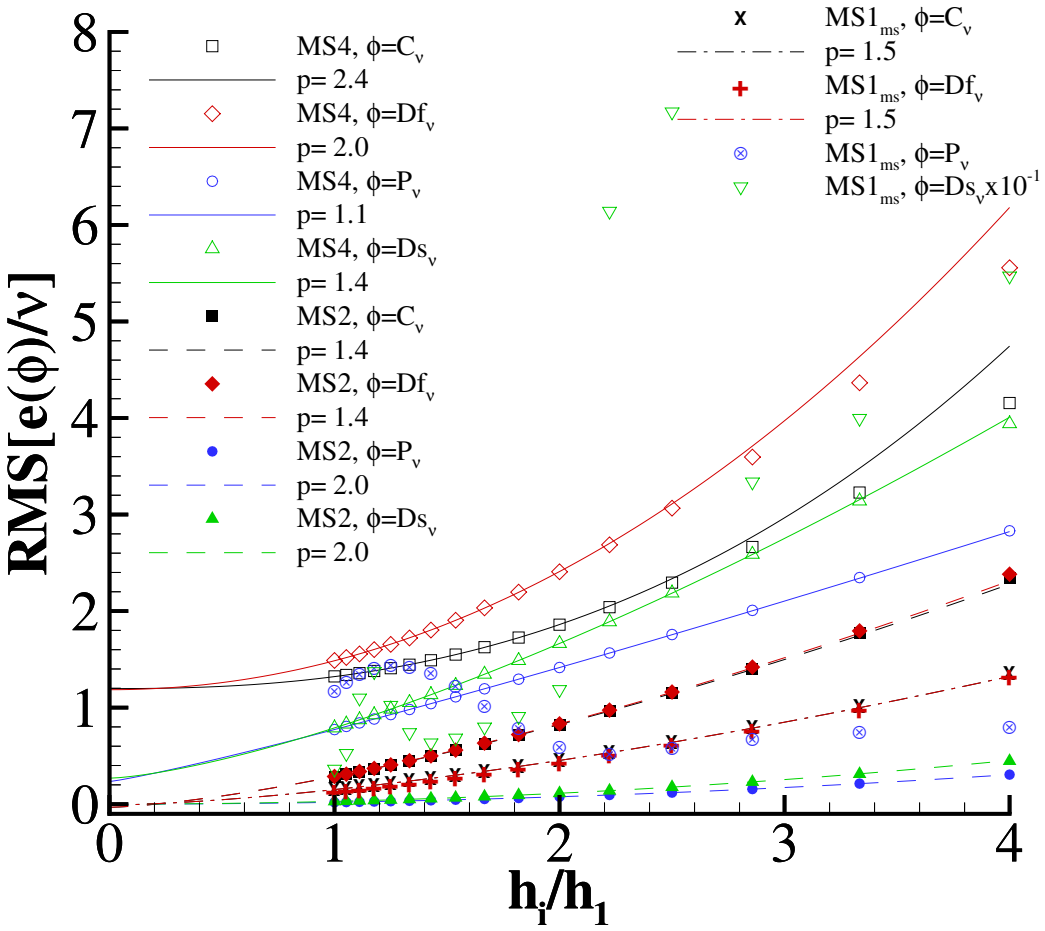

Figure 4: Convergence of the RMS of the error of the terms of the $\tilde{\nu}$ transport equation with the grid refinement in grid set ST1. Spalart & Allmaras one-equation model.

- The convergence of the RMS of the error of the dissipation term is erratic. The convergence of the production term is also non-monotonic, but clearly smoother than the one obtained for dissipation. This explains the difficulties to converge the numerical solution when these terms are also solved numerically.

- The origin of the problem is the near-bottom behaviour of the dissipation term in the MS1. In the Spalart & Allmaras model, dissipation is proportional to the ratio $\tilde{\nu}$ divided by y squared. In the MS4 and MS2 cases, this quantity goes to zero at the bottom of the domain. However, in the MS1 the ratio of $\tilde{\nu}$ by y is independent of y and it exhibits a large

value close to the bottom. Any small error in $\tilde{\nu}$ will be amplified significantly in the dissipation term. These results are confirmed by the smooth convergence behaviour obtained at most of the 8 selected locations of the three grid sets. Furthermore, the Eq set which includes the grids with the largest near-bottom grid line spacing exhibit much weaker convergence problems than the ST1 and ST2 sets.

– With the production and dissipation term imposed from the MS, convection and diffusion exhibit the expected behaviour for the MS1.

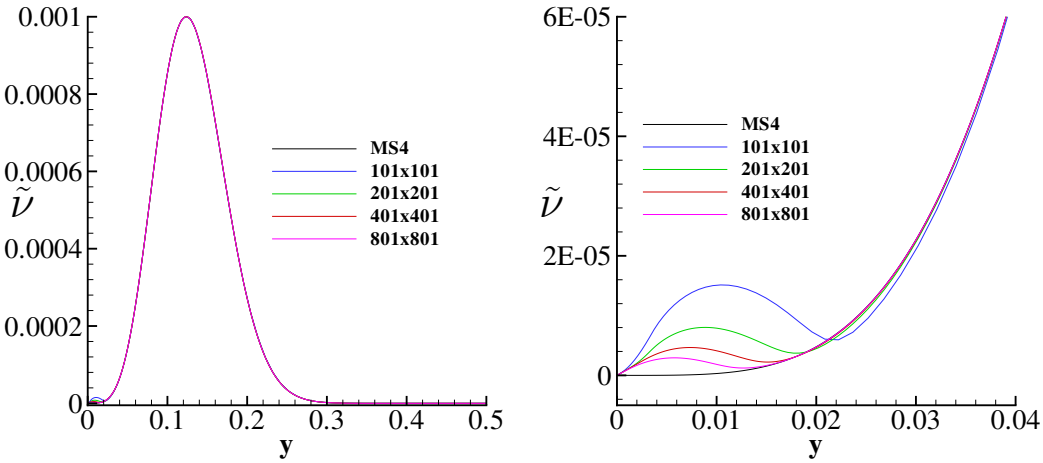

Figure 5: $\tilde{\nu}$ profiles at $x = 0.875$ in grid set ST1. Spalart & Allmaras one-equation model with the MS4.

- MS4 case

  – This case exhibits a very awkward behaviour of the RMS of the error of convection and diffusion. There is a clear dependence of p on the groups of grids selected and the extrapolation of the error of C_ν and Df_ν to cell size is not zero. However, this dependency does not appear at the 8 selected locations of the grid set. On the other hand, production and dissipation exhibit a p for the RMS of the error which is independent of the groups of grid selected. However, the extrapolated values to cell size zero are still incoherent.

  – As illustrated in [8], the strange results obtained for the MS4 are a consequence of the near-bottom behaviour of the solution. Figure 5 presents the $\tilde{\nu}$ profiles at $x = 0.875$ for 4 grids of the ST1 set. In

this plot we have included an extra level of grid refinement, 801×801. The data plotted in figure 5 show that there is an oscillation in the calculated profiles in the near-bottom region that disappears very slowly with the grid refinement. This oscillation increases with the distance to the inlet, i.e. a similar comparison for $x < 0.875$ exhibits smaller differences between the MS's and the four calculated profiles than the lines plotted in figure 5. In the near-bottom region, the MS changes with y^4 and the present solver is only second-order accurate.

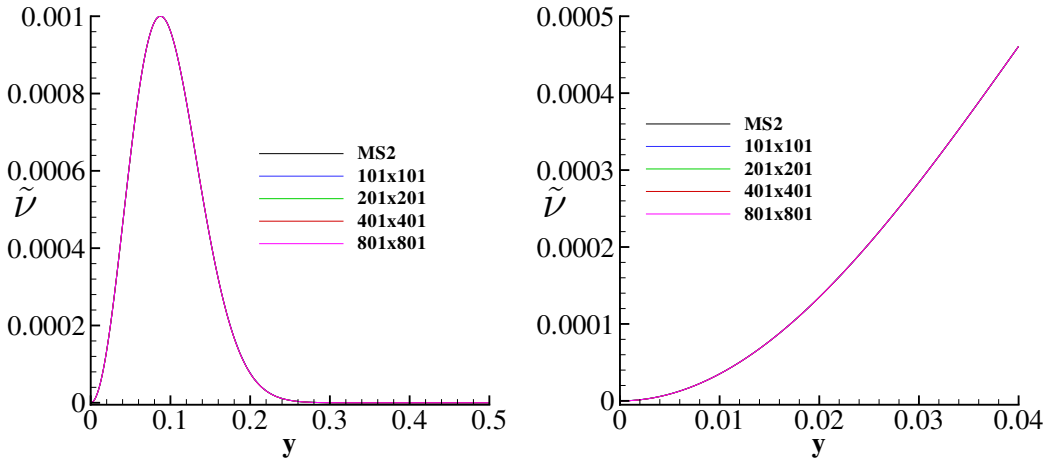

Figure 6: $\tilde{\nu}$ profiles at $x = 0.875$ in grid set ST1. Spalart & Allmaras one-equation model with the MS2.

For the sake of completeness, the $\tilde{\nu}$ profiles at $x = 0.875$ for the MS2 and MS1 are presented in figures 6 and 7. In these two cases, the near-bottom solutions converge smoothly. However, we must emphasize once more that the MS1 solution is not a good option for the Spalart & Allmaras model.

The convergence properties of $\tilde{\nu}$ with the three MS's show that the observed order of accuracy obtained in the solution of the $\tilde{\nu}$ transport equation may not correspond to the theoretical order of the method adopted. However, in practical applications the objective of the turbulence model is to compute the eddy-viscosity, ν_t. Therefore, it is important to check the convergence properties of ν_t. In the Spalart & Allmaras model, ν_t is calculated from the product of $\tilde{\nu}$ by the damping function, f_{v1}.

Figure 8 presents the RMS of the error of ν_t for the MS4, MS2 and MS1 in the three grid sets, Eq, ST1 and ST2. The observed order of accuracy of ν_t for the RMS of the error and of the 8 selected locations of each set are presented in tables 10 to 12 of appendix A.

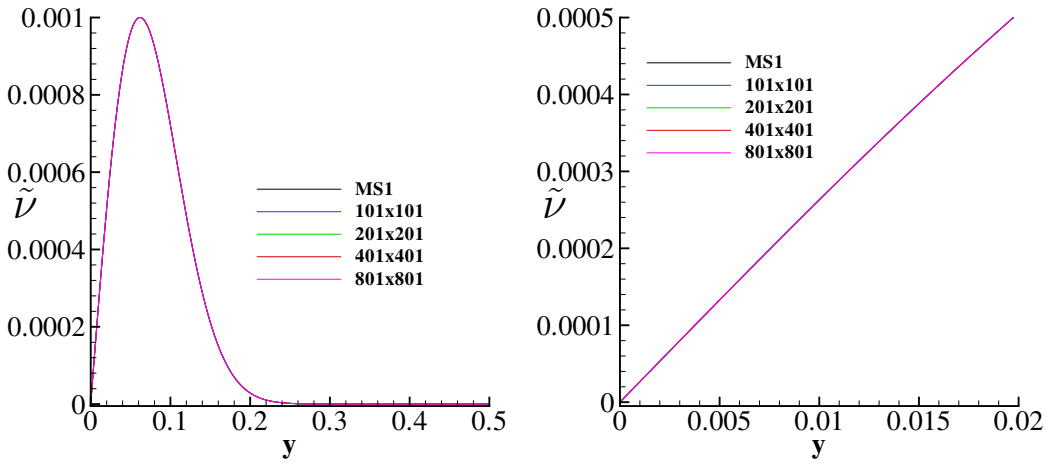

Figure 7: $\tilde{\nu}$ profiles at $x = 0.875$ in grid set ST1. Spalart & Allmaras one-equation model with the MS1. Production and dissipation terms imposed from the MS.

The data presented in figure 8 and tables 10 to 12 suggest the following remarks:

- The results obtained for ν_t are very similar to the ones plotted in figure 3 for $\tilde{\nu}$. However, the error level is slightly smaller for ν_t than for $\tilde{\nu}$.
- The results of ν_t at the selected locations of grid set Eq are equivalent to those of $\tilde{\nu}$, because all the 8 selected locations are in a region where the damping function is inactive, $f_{v1} = 1$.
- For the ST1 grid set, the observed order of accuracy of ν_t is significantly larger than the p of $\tilde{\nu}$ for the MS4. However, with the other two MS's p is fairly similar for both variables.
- The grid set with the locations closest to the bottom (smallest values of f_{v1}) is grid set ST2. The values of p for ν_t in this grid set are substantially different than the ones obtained for $\tilde{\nu}$ in most cases.

As an example of the influence of f_{v1} in the convergence properties of ν_t, figure 9 presents the convergence with the grid refinement of ν_t and $\tilde{\nu}$ at three selected locations of set ST1.

In two of the three locations presented, the error of ν_t is smaller than the error of $\tilde{\nu}$ for the same grid density. The exception is the MS1 case, where the higher level of $\tilde{\nu}$ close to the bottom makes the damping function almost 1 at the selected location. Nevertheless, the MS4 solution exhibits different values of p for ν_t and

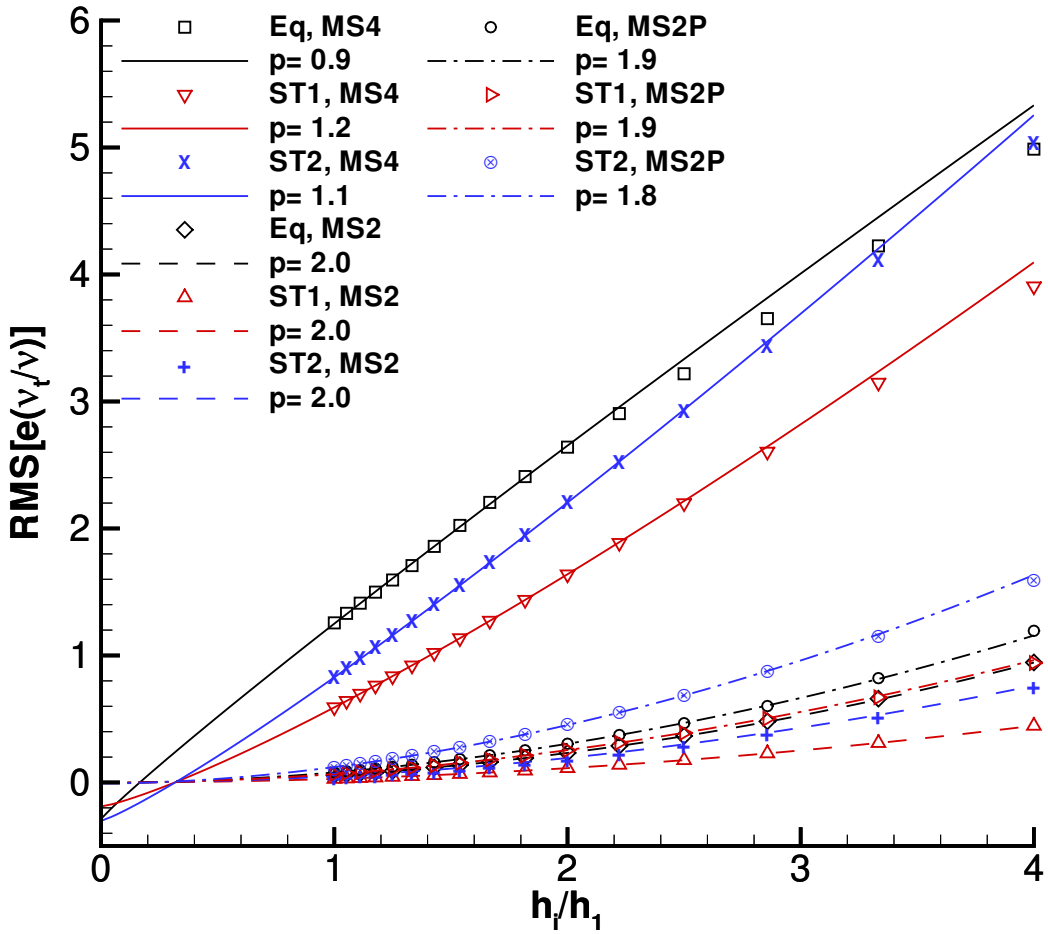

Figure 8: Convergence of the RMS of the error of ν_t with the grid refinement in the grid sets Eq, ST1 and ST2. Spalart & Allmaras one-equation model.

$\tilde{\nu}$. This change of p between $\tilde{\nu}$ and ν_t is a direct consequence of the damping function, f_{v1}. In the other two MS's, the observed order of accuracy of ν_t is equal to the p for $\tilde{\nu}$.

It is important to investigate the effect of the poor convergence of $\tilde{\nu}$ obtained with the MS4 in the near-bottom region in the ν_t profile. In this region the damping function, f_{v1}, tends to zero and so the oscillations present in the $\tilde{\nu}$ profiles may be damped for the eddy-viscosity field. Figure 10 presents the near-bottom eddy-viscosity profiles for the MS4 at $x = 0.875$. To simplify the comparison, the $\tilde{\nu}$ profiles (presented in figure 5) are also plotted in figure 10.

The results show that the oscillations in the ν_t profiles are clearly damped in

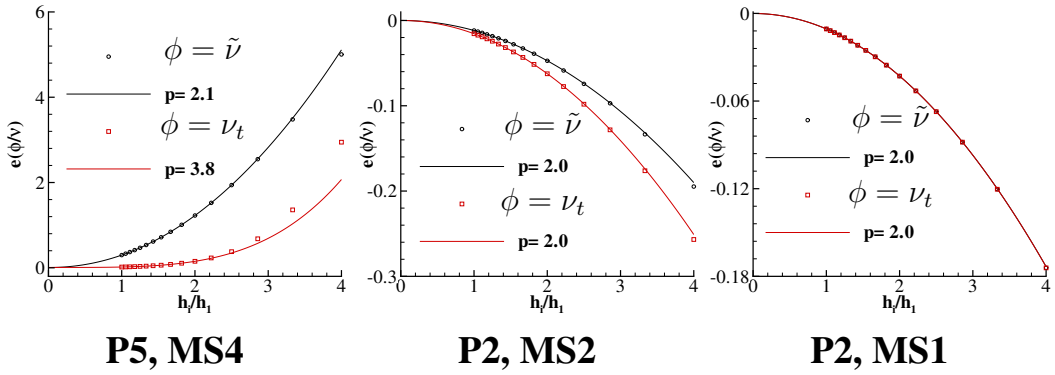

Figure 9: Convergence of ν_t and $\tilde{\nu}$ with the grid refinement at selected locations of the grid set ST1. Spalart & Allmaras one-equation model.

the near-bottom region. However, for the coarsest grids there is still a significant error in the ν_t profile, which leads to a poor convergence of the flow field with the Spalart & Allmaras turbulence model as reported in [8].

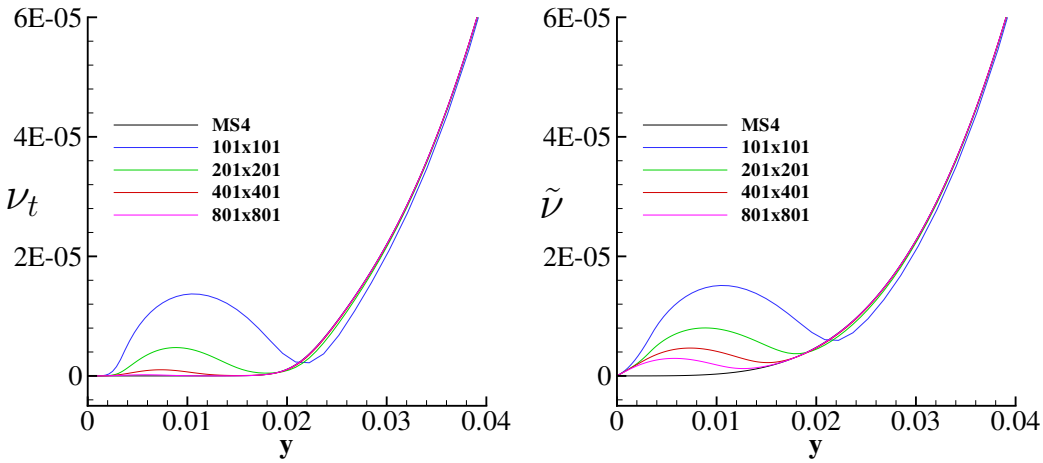

Figure 10: ν_t and $\tilde{\nu}$ profiles at $x = 0.875$ in the near-bottom region for the MS4 in grid set ST1. Spalart & Allmaras one-equation model.

4.4.3 Menter one equation model

The one equation model proposed by Menter in [3] is similar to the Spalart & Allmaras model. The two main differences between the two models is the

dissipation term and the formulation of the damping function. Therefore, one would expect a performance of the numerical solution of the transport equation of Menter's model with the manufactured velocity field similar (with the possible exception of the MS1) to the one discussed above for the Spalart & Allmaras. However, that is not the case.

Although there are several differences between the results of the two models that we will discuss below, there are two significant changes in the numerical performance of the Menter model for the three MS's when compared to the Spalart & Allmaras model:

1. In the Menter model, the MS2 leads to an unstable numerical solution. The origin of the problem is the production term that tends to zero close to the bottom resulting in negative values for $\tilde{\nu}_t$. In PARNASSOS, [9], unphysical negative turbulence quantities are not allowed and so the calculations are interrupted. Instead of modifying the code to accept negative values of $\tilde{\nu}_t$ (this would only be useful in the context of Method of the Manufactured Solutions), we have assumed that the production term is exact for the solution of the MS2 (as we have done for the MS1 with the Spalart & Allmaras model), i.e. the production term is defined by the manufactured flow quantities. Therefore, we will designate the MS2 case by MS2$_{mp}$ for Menter's model.

2. There are no convergence problems for the MS1 with Menter's model. The different formulation of the dissipation term in this one-equation turbulence model must be responsible for this result.

The convergence of the RMS of the error of $\tilde{\nu}_t$ as a function of the grid refinement is presented in figure 11. Tables 13 to 15 present the values of p for the error of $\tilde{\nu}_t$ at the 8 selected locations of each set and for the RMS of the error of $\tilde{\nu}_t$ for different groups of grids.

The convergence properties obtained for the Menter model are not equal to the ones exhibited by the Spalart & Allmaras model results. However, there are some similarities between the data obtained with the two models.

- As for the Spalart & Allmaras model, the MS4 leads to the least regular convergence of $\tilde{\nu}$. The observed order of accuracy exhibited by the Menter model is clearly larger than for the Spalart & Allmaras model. However, the extrapolation to cell size zero in not consistent.

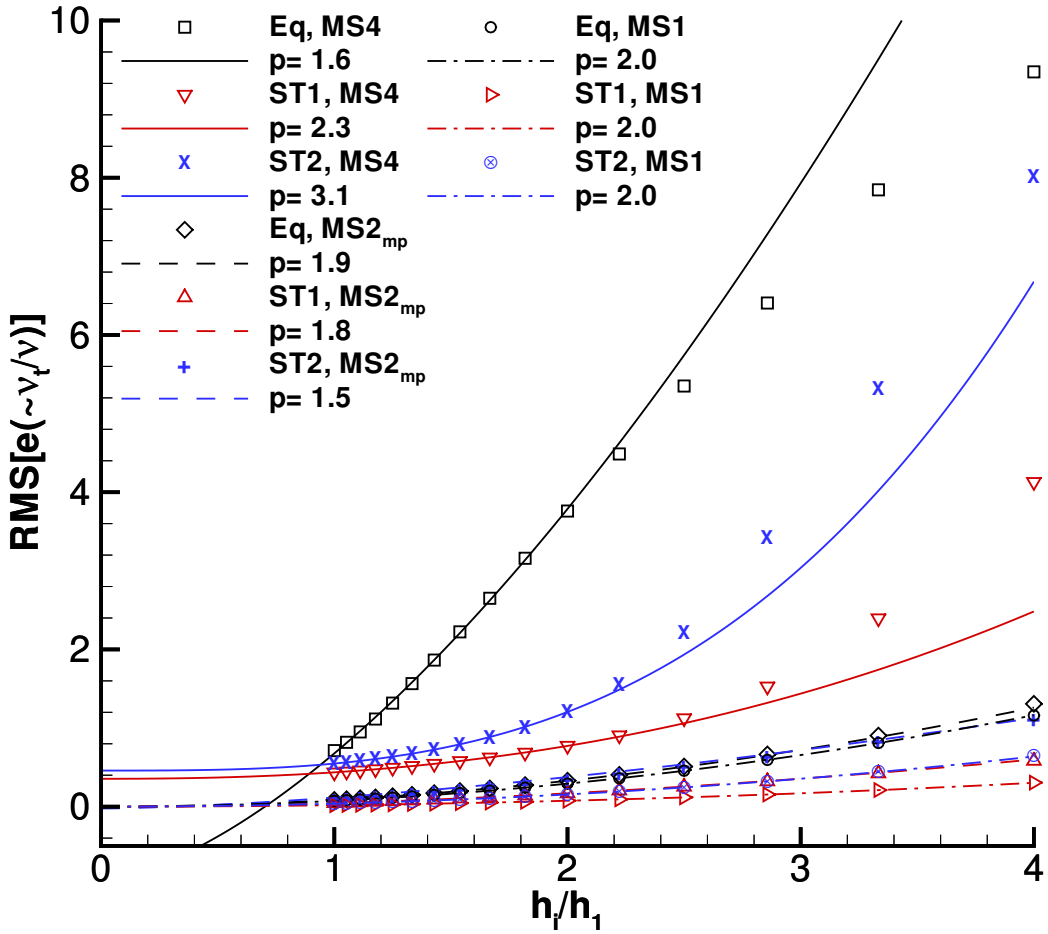

Figure 11: Convergence of the RMS of the error of $\tilde{\nu}_t$ with the grid refinement in the grid sets Eq, ST1 and ST2. Menter one-equation model.

- There is a large percentage of the local solutions that shows a value of p nearly independent of the groups of grids selected. However, the RMS of the error does not reflect this behaviour in several cases. This indicates that the observed order of accuracy is clearly dependent on the location selected.

- The most consistent results are obtained for the MS1 case, which exhibits exactly the theoretical order of the method. In the MS2$_{mp}$ there is a slight dependency of p on the grid set selected. This is a peculiar result, because the MS with the best performance in Menter's model is the one that leads to the most complicated numerical problems for the Spalart & Allmaras model.

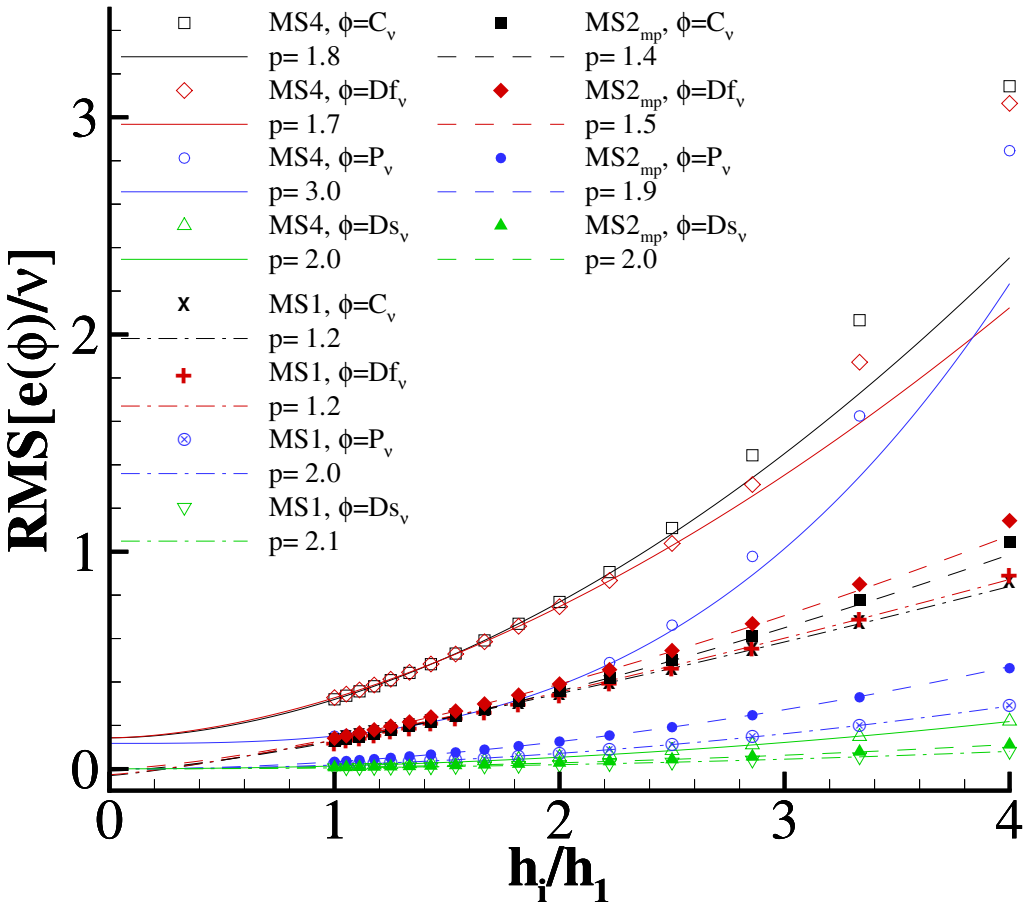

Figure 12: Convergence of the RMS of the error of the terms of the $\tilde{\nu}$ transport equation with the grid refinement in grid set ST1. Menter one-equation model.

As for the Spalart & Allmaras model, we have investigated the convergence of the four terms of the $\tilde{\nu}_t$ transport equation, which are given by:

1. Convection, C_ν.

$$u\frac{\partial \tilde{\nu}_t}{\partial x} + v\frac{\partial \tilde{\nu}_t}{\partial y}$$

2. Diffusion, Df_ν.

$$-\nabla \cdot \left((\nu + \frac{\tilde{\nu}_t}{\sigma}) \nabla \tilde{\nu}_t \right)$$

3. Production, P_ν.

$$-c_1 D_1 \tilde{\nu}_t \sqrt{S}$$

4. Dissipation, Ds_ν.

$$c_2 E_{1e}$$

Tables 16 to 19 of appendix A present the values of p for the error of C_ν, Df_ν, P_ν and Ds_ν at the 8 selected locations of the set ST1. The tables include also the observed order of accuracy of the RMS of the error, which is presented in figure 12 as a function of the grid refinement level for the grid set ST1. The comparison with the results obtained for the Spalart & Allmaras model (plotted in figure 4) show two main differences:

- The convergence in the case MS4 is better for the Menter model than for the Spalart & Allmaras model. The values of p for convection and diffusion are less dependent on the groups of grids selected and its value is closer to the theoretical order of the method. However, the extrapolation to cell size zero is still inconsistent.

- As for the Spalart & Allmaras model, none of the MS's exhibits the same order of accuracy for the four terms of the dependent variable transport equation. Nevertheless, the results obtained with the MS1 and MS2 are very similar. However, the MS2 required the use of the manufactured production term to avoid numerical problems.

It is interesting to remark that the single term that exhibits a consistent order of accuracy in all the MS's is dissipation. This is probably a consequence of the frozen velocity field and of the second order accurate discretization of the gradient of the strain rate.

The calculation of the MS2$_{mp}$ required the use of the exact production term to obtain a stable solution. Nevertheless, we have computed the error of the production term from the converged solutions. It is impressive (to say the least) that an error which is clearly below the two main contributions, convection and diffusion, may deteriorate so drastically the numerical convergence of the solution of the $\tilde{\nu}_t$ transport equation. However, one must not forget that several terms (in the present context convection is a linear term) of the $\tilde{\nu}_t$ transport equation are not linear.

The $\tilde{\nu}_t$ profiles at $x = 0.875$ for the MS4, MS2$_{mp}$ and MS1 are plotted in figure 13 for 4 grids of the ST1 set. The data plotted in figure 13 suggest the following remarks:

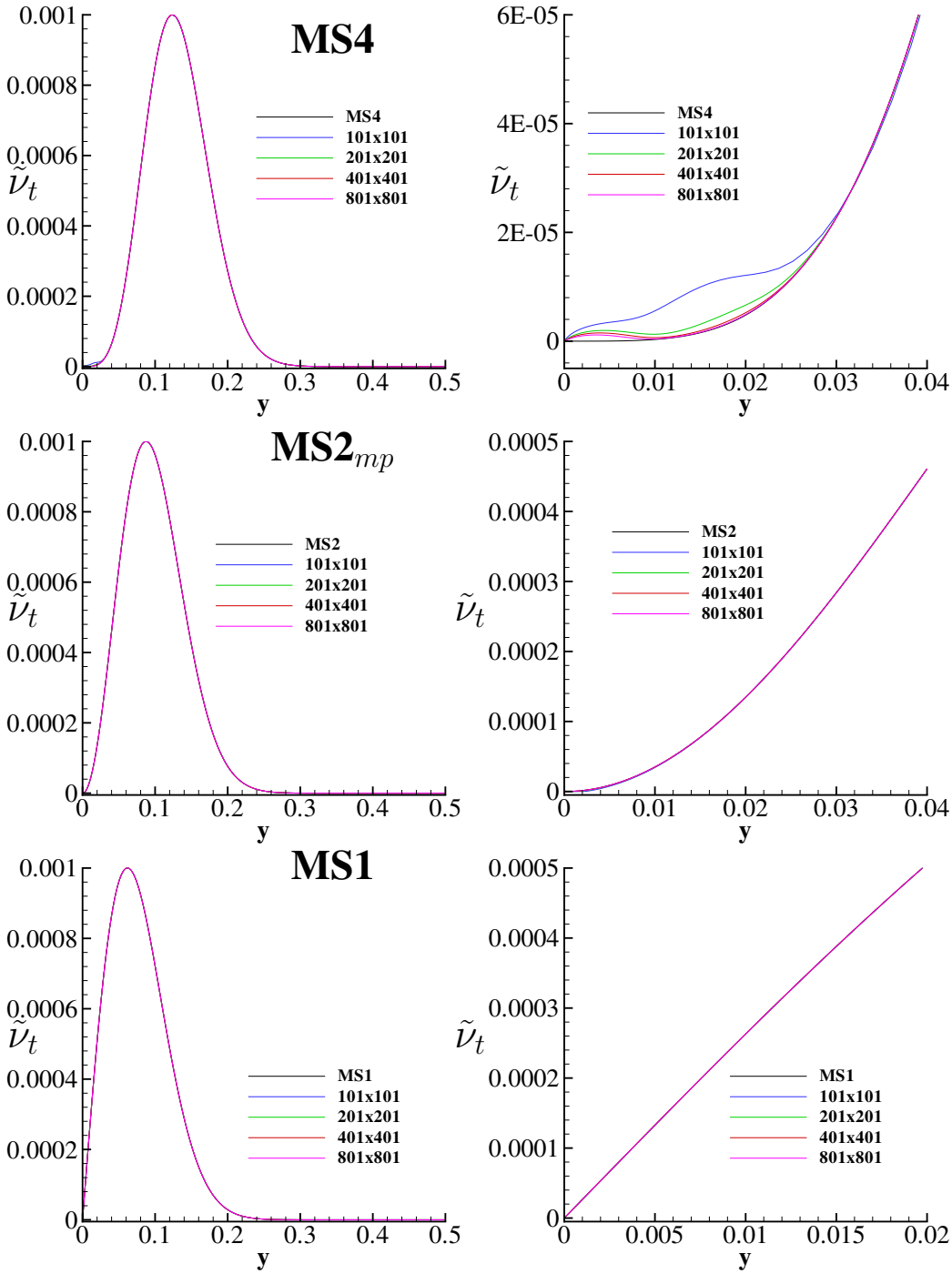

Figure 13: $\tilde{\nu}$ profiles at $x = 0.875$ in grid set ST1. Menter one-equation model with the MS4, MS2$_{mp}$ and MS1.

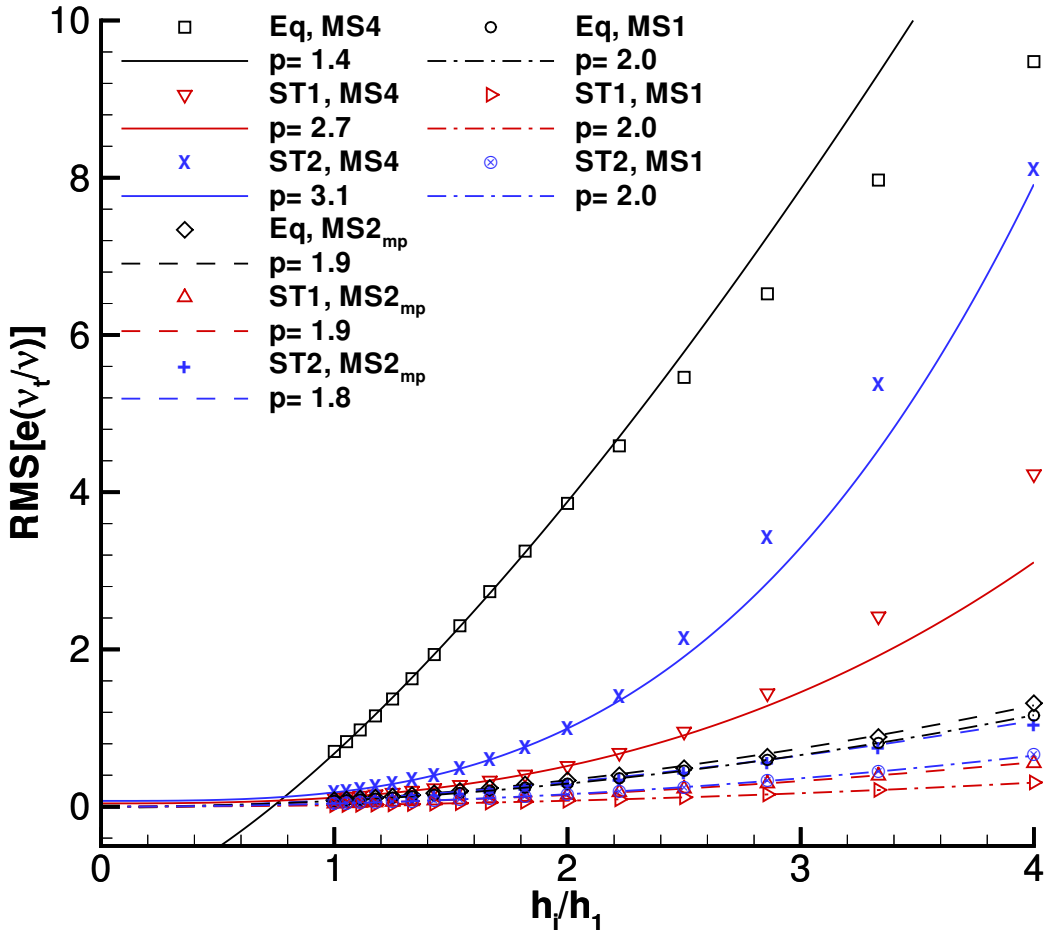

Figure 14: Convergence of the RMS of the error of ν_t with the grid refinement in the grid sets Eq, ST1 and ST2. Menter one-equation model.

- As expected, the oscillation in the near-bottom region is also present in the MS4. However, in Menter's model the errors are smaller than in Spalart & Allmaras model. On the other hand, the region with "visible" error is wider in the Menter model than in the Spalart & Allmaras model.

- As for the Spalart & Allmaras model, the numerical solutions of the MS2$_{mp}$ are perfectly smooth. However, one should not forget that the Menter model required the exact production term to obtain converged solutions. Therefore, the performance of the two equation models for this MS is also different.

- The $\tilde{\nu}_t$ profiles for the MS1 are perfectly smooth. The performance of the

two models is still different, because the MS1 is the most troublesome MS for the Spalart & Allmaras model.

As for the Spalart & Allmaras model, we have also investigated the convergence of ν_t for the Menter model. Tables 20, 21 and 22 include the observed order of accuracy of the convergence of ν_t at the 8 selected locations of each grid set. The tables also include the p of the RMS of the error of ν_t. Figure 14 presents the RMS of the error of ν_t as a function of the grid refinement.

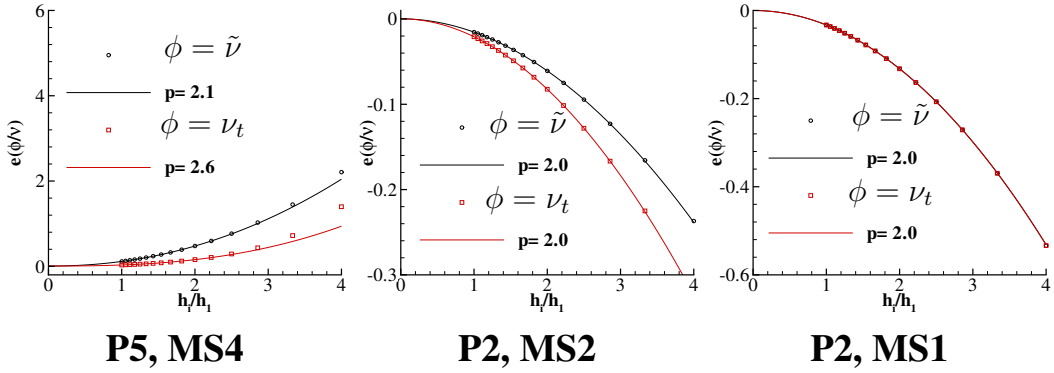

Figure 15: Convergence of ν_t and $\tilde{\nu}$ with the grid refinement at selected locations of the grid set ST1. Menter one-equation model.

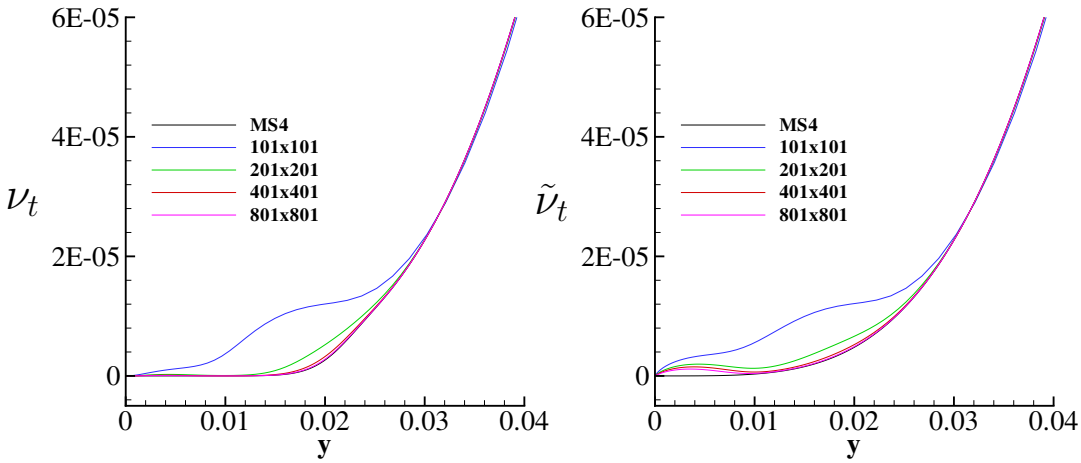

Figure 16: ν_t and $\tilde{\nu}$ profiles at $x = 0.875$ in the near-bottom region for the MS4 in grid set ST1. Menter one-equation model.

As for $\tilde{\nu}_t$, there is a significant influence of the grid set selected in the convergence properties (error level and p) obtained for the MS4. The comparison

of the convergence properties of ν_t and $\tilde{\nu}_t$ of the Menter model is similar to the one discussed above for ν_t and $\tilde{\nu}$ of the Spalart & Allmaras model. However, the convergence of ν_t in the two one-equation models is significantly different. Nevertheless, the comparison of the convergence of $\tilde{\nu}_t$ and ν_t of the Menter model, figure 15, at the same selected locations included in figure 9 for the Spalart & Allmaras model is qualitatively similar to the one of the Spalart & Allmaras model.

With the Menter model, the MS4 also leads to oscillations in the $\tilde{\nu}_t$ profiles close to the bottom of the domain. Therefore, we have plotted in figure 16 the ν_t and $\tilde{\nu}_t$ profiles at $x = 0.875$ for the MS4 in the ST1 grid set. As expected, the oscillation in the ν_t profiles are damped by the function, D_2. However, the damping is not sufficient to avoid poor convergence properties for the calculations with the complete flow field.

5 Conclusions

This report presents three manufactured solutions for the one-equation turbulence models of Spalart & Allmaras and Menter. The velocity and pressure field are common to the three solutions, which differ in the specification of the dependent variable of the turbulence model.

As a first check of the proposed manufactured solutions, the transport equation of the two turbulence models has been solved with a frozen velocity field, i.e. the manufactured velocity field. The results obtained with this exercise showed an unexpected sensitivity of the one-equation models to the manufactured field of the dependent variable. Furthermore, none of the three MS's presented leads to a similar behaviour of the two one-equation models tested.

The original MS proposed in [1] leads to convergence difficulties near the bottom of the computational domain, which are linked to the dependence of the manufactured solution on the fourth power of the distance to the bottom.

The proposed MS with a y^2 dependence in the "near-wall" region significantly improves the convergence properties of the Spalart & Allmaras model. However, it leads to an unstable solution in the Menter model. The instabilities are originated by the production term.

On the other hand, the MS that has a linear variation with the distance to the bottom leads to the best convergence properties of the Menter model and to the most severe numerical problems of the Spalart & Allmaras model. In this case, the dissipation term is responsible for the numerical instabilities.

The grid dependency studies performed for the three MS's presented also some difficulties for error estimation procedures:

- The convergence properties (error level and observed order of accuracy) are strongly dependent on the behaviour of the dependent variable of the two turbulence models. Furthermore, the observed order of accuracy of the turbulence quantities may be significantly different from the theoretical order of the numerical method adopted.
- In general, the observed order of accuracy of the turbulence quantities is not uniform for the complete flow field. This means that the observed order of accuracy of the RMS may not be representative of the local convergence properties.
- The convergence properties of the eddy-viscosity may be affected by the damping functions of the model.

The results presented in this study suggest that it is likely that the numerical properties of the transport equations of the one-equation turbulence models tested will be a disturbing factor in error estimation for complex turbulence flows. Unless, one decides to adopt the "philosophy" of Brian Launder in his book: "Turbulence modelling is the triumph of hope over experience"...

References

[1] Eça L., Hoekstra M., Hay A., Pelletier D. - *A Manufactured Solution for a Two-Dimensional Steady Wall-Bounded Incompressible Turbulent Flow* - IST Report D72-34, EPM Report EMP-RT-2005-08, November 2005.

[2] Spalart P.R., Allmaras S.R. - *A One-Equations Turbulence Model for Aerodynamic Flows* - AIAA 30th Aerospace Sciences Meeting, Reno, January 1992.

[3] Menter F.R. - *Eddy-Viscosity Transport Equations and their Relation to the* $k-\epsilon$ *Model* - Journal of Fluids Engineering, Vol. 119, December 1997, pp. 876-884.

[4] Launder B.E., Spalding - *The numerical computation of turbulent flows* - Computer Methods in Applied Mechanics and Engineering, Vol. 3, N^{o}2, 1974, pp. 269-289.

[5] Chien K.Y - *Prediction of Channel and Boundary-Layer Flows with a Low-Reynolds-Number Turbulence Model.* - AIAA Journal, Vol. 20, January 1982, pp. 33-38.

[6] Kok J.C. - *Resolving the Dependence on Free-stream values for the $k-\omega$ Turbulence Model* - NLR-TP-99295, 1999.

[7] Menter F.R. - *Two-Equation Eddy-Viscosity Turbulence Models for Engineering Applications* - AIAA Journal, Vol.32, August 1994, pp. 1598-1605.

[8] Eça L. - *Calculation of a Manufactured Solution for a 2-D Steady Incompressible Near-Wall Turbulent Flow with PARNASSOS* - IST Report D72-35, January 2006.

[9] José M.Q.B. Jacob, Eça L. - *2-D Incompressible Steady Flow Calculations with a Fully Coupled Method* - VI Congresso Nacional de Mecânica Aplicada e Computacional, Aveiro, April 2000

[10] Saad Y, Schultz M.H. - *GMRES: a generalized minumum residual algorithm for solving nonsymmetric linear systems* - SIAM Jnl. Sci. Statist. Comp., Vol. 7, pp 856-869, 1986.

[11] Vinokur M. - *On One-Dimensional Stretching Functions for Finite-Difference Calculations.* - Journal of Computational Physics, Vol. 50, 1983, pp. 215-234.

[12] Roache P.J. - *Verification and Validation in Computational Science and Engineering* - Hermosa Publishers, 1998.

[13] Eça L, Hoekstra M., *An Evaluation of Verification Procedures for CFD Applications*, 24^{th} Symposium on Naval Hydrodynamics, Fukuoka, Japan, July 2002.

A Observed order of accuracy of the turbulence quantities for different groups of grids

A.1 Spalart & Allmaras one-equation model

This section presents the values of p as a function of the number of grids selected for the following flow variables:

- Dependent variable of the model, $\tilde{\nu}$.
  - Grid set Eq.
  - Grid set ST1.
  - Grid set ST2.
- Convection terms of the $\tilde{\nu}$ transport equation.
  - Grid set ST1.
- Diffusion terms of the $\tilde{\nu}$ transport equation.
  - Grid set ST1.
- Production terms of the $\tilde{\nu}$ transport equation.
  - Grid set ST1.
- Dissipation term of the $\tilde{\nu}$ transport equation.
  - Grid set ST1.
- Eddy-viscosity, ν_t.
  - Grid set Eq.
  - Grid set ST1.
  - Grid set ST2.

	Grids	r_{i1}	P1	P2	P3	P4	P5	P6	P7	P8	L_2
	1- 6	1.33	2.1	2.0	2.0	2.0	2.0	2.0	1.9	2.6	0.8
	1- 7	1.43	2.1	2.0	2.0	2.0	2.0	2.0	1.9	2.6	1.5
	1- 8	1.54	2.1	2.0	1.9	2.0	2.0	2.0	1.9	2.7	1.6
	1- 9	1.67	2.1	2.0	1.9	2.0	2.0	2.0	1.9	2.7	1.4
	1-10	1.82	2.2	2.0	1.9	2.0	2.0	2.0	1.9	2.7	1.2
MS4	1-11	2.00	2.2	2.0	1.9	2.0	2.0	2.0	1.8	2.7	1.0
	1-12	2.22	2.2	2.0	1.9	1.9	1.9	1.9	1.8	2.7	0.8
	1-13	2.50	2.2	2.0	1.9	1.9	1.9	1.9	1.8	2.7	0.8
	1-14	2.86	2.2	2.0	1.9	1.9	1.9	1.9	1.8	2.8	0.8
	1-15	3.33	2.3	2.0	1.9	1.9	1.9	1.9	1.7	2.8	0.8
	1-16	4.00	2.3	2.1	1.9	1.9	1.9	1.9	1.7	2.8	0.9
	1- 6	1.33	2.0	2.0	2.0	2.0	1.9	0.6	2.0	1.8	2.0
	1- 7	1.43	2.0	2.0	2.0	2.0	1.9	0.5	2.0	1.8	2.0
	1- 8	1.54	2.0	2.0	2.0	2.0	1.9	0.3	2.0	1.8	2.0
	1- 9	1.67	2.0	2.0	2.0	2.0	1.9	0.0	2.0	1.8	2.0
	1-10	1.82	2.0	2.0	2.0	2.0	1.9	0.0	2.0	1.8	2.0
MS2	1-11	2.00	2.0	2.0	2.0	2.0	1.9	0.0	2.0	1.8	2.0
	1-12	2.22	2.0	2.0	2.0	2.0	1.9	0.0	2.0	1.8	2.0
	1-13	2.50	2.0	2.0	2.0	2.0	1.9	0.0	2.0	1.8	2.0
	1-14	2.86	2.0	2.0	2.0	2.0	1.9	0.0	2.0	1.7	2.0
	1-15	3.33	2.0	2.0	2.0	2.0	1.9	—	2.0	1.7	2.0
	1-16	4.00	2.1	2.0	2.0	2.0	1.8	6.3	2.0	1.7	2.0
	1- 6	1.33	2.0	2.0	2.0	2.0	0.0	2.0	1.8	0.8	2.0
	1- 7	1.43	2.0	2.0	2.0	2.0	0.0	2.0	1.8	0.7	2.0
	1- 8	1.54	2.0	2.0	2.0	1.9	0.0	2.0	1.8	0.6	2.0
	1- 9	1.67	2.0	2.0	2.0	1.9	0.0	2.0	1.8	0.4	2.0
	1-10	1.82	2.0	2.0	2.0	1.9	0.0	2.0	1.8	0.1	2.0
$MS1_{ms}$	1-11	2.00	2.0	2.0	2.0	1.9	0.0	2.0	1.7	0.0	2.0
	1-12	2.22	2.0	2.0	2.0	1.9	—	2.0	1.7	0.0	2.0
	1-13	2.50	2.0	2.0	2.0	1.9	—	2.0	1.7	0.0	2.0
	1-14	2.86	2.0	2.0	2.0	1.9	7.9	2.0	1.6	0.0	2.0
	1-15	3.33	2.0	2.0	2.0	1.9	6.0	2.0	1.6	—	2.0
	1-16	4.00	2.1	2.0	2.0	1.9	5.0	2.0	1.5	7.5	2.0

Table 3: Observed order of accuracy of $\tilde{\nu}$ at the 8 selected locations of set Eq. Spalart & Allmaras one-equation turbulence model.

	Grids	r_{i1}	P1	P2	P3	P4	P5	P6	P7	P8	L_2
	1- 6	1.33	2.0	2.0	2.1	2.0	2.1	0.7	2.0	2.0	1.0
	1- 7	1.43	2.0	2.0	2.1	2.0	2.1	0.5	2.0	2.0	1.0
	1- 8	1.54	2.0	2.0	2.1	2.0	2.1	0.2	2.0	2.1	1.0
	1- 9	1.67	2.0	2.0	2.1	2.0	2.1	0.0	2.0	2.1	1.0
	1-10	1.82	2.0	2.0	2.1	2.0	2.1	0.0	2.0	2.1	1.0
MS4	1-11	2.00	2.0	2.0	2.2	2.0	2.1	0.0	2.0	2.1	1.0
	1-12	2.22	2.0	2.0	2.2	2.0	2.1	0.0	2.0	2.1	1.0
	1-13	2.50	2.0	2.1	2.2	2.0	2.1	—	2.0	2.1	1.0
	1-14	2.86	2.0	2.1	2.3	1.9	2.1	—	2.0	2.1	1.1
	1-15	3.33	2.0	2.1	2.3	1.9	2.0	7.4	2.0	2.1	1.1
	1-16	4.00	2.0	2.1	2.4	1.9	2.0	5.9	2.0	2.1	1.0
	1- 6	1.33	1.8	2.0	2.0	2.1	2.1	2.1	2.1	2.2	2.0
	1- 7	1.43	1.9	2.0	2.0	2.1	2.1	2.1	2.1	2.2	2.0
	1- 8	1.54	2.1	2.0	2.0	2.1	2.1	2.1	2.1	2.2	2.0
	1- 9	1.67	1.9	2.0	2.0	2.1	2.1	2.1	2.1	2.2	2.0
	1-10	1.82	1.8	2.0	2.0	2.1	2.1	2.2	2.2	2.2	2.0
MS2	1-11	2.00	2.0	2.0	2.0	2.1	2.1	2.2	2.2	2.2	2.0
	1-12	2.22	1.8	2.0	2.0	2.1	2.2	2.2	2.2	2.2	2.0
	1-13	2.50	1.7	2.0	2.0	2.1	2.2	2.2	2.2	2.2	2.0
	1-14	2.86	1.9	2.0	2.1	2.1	2.2	2.2	2.2	2.2	2.0
	1-15	3.33	1.7	2.0	2.1	2.1	2.2	2.2	2.2	2.3	2.0
	1-16	4.00	1.6	2.1	2.1	2.1	2.2	2.2	2.2	2.3	2.0
	1- 6	1.33	2.0	2.0	2.1	1.8	1.9	2.0	2.0	2.0	2.0
	1- 7	1.43	2.0	2.0	2.1	1.8	1.9	2.0	2.0	2.0	2.0
	1- 8	1.54	2.0	2.0	2.1	1.8	1.9	2.0	2.0	2.0	2.0
	1- 9	1.67	2.0	2.0	2.1	1.8	1.9	2.0	2.0	2.0	2.0
	1-10	1.82	2.0	2.0	2.1	1.8	1.9	2.0	2.0	2.0	2.0
$MS1_{ms}$	1-11	2.00	2.0	2.0	2.1	1.8	1.9	2.0	2.0	2.0	2.0
	1-12	2.22	2.0	2.0	2.1	1.8	1.9	1.9	2.0	2.0	2.0
	1-13	2.50	2.0	2.0	2.1	1.7	1.9	1.9	2.0	2.0	2.0
	1-14	2.86	2.0	2.0	2.1	1.7	1.9	1.9	2.0	2.0	2.0
	1-15	3.33	2.0	2.0	2.1	1.7	1.9	1.9	2.0	2.0	2.0
	1-16	4.00	2.0	2.0	2.1	1.6	1.9	1.9	1.9	2.0	2.0

Table 4: Observed order of accuracy of $\tilde{\nu}$ at the 8 selected locations of set ST1. Spalart & Allmaras one-equation turbulence model.

	Grids	r_{i1}	P1	P2	P3	P4	P5	P6	P7	P8	L_2
	1- 6	1.33	2.0	2.1	2.3	1.3	0.0	0.2	1.0	0.9	1.1
	1- 7	1.43	2.0	2.1	2.3	1.2	0.0	0.3	1.0	0.9	1.1
	1- 8	1.54	2.0	2.1	2.3	1.1	0.0	0.3	1.1	0.9	1.1
	1- 9	1.67	2.0	2.1	2.3	0.9	0.0	0.4	1.1	0.9	1.1
	1-10	1.82	2.0	2.1	2.4	0.8	0.0	0.4	1.1	0.9	1.1
MS4	1-11	2.00	2.0	2.1	2.4	0.6	0.0	0.5	1.2	0.9	1.1
	1-12	2.22	2.0	2.1	2.4	0.5	0.0	0.5	1.2	0.9	1.1
	1-13	2.50	2.0	2.1	2.4	0.3	0.0	0.7	1.2	0.9	1.1
	1-14	2.86	2.0	2.1	2.4	0.1	0.0	1.0	1.2	0.8	1.1
	1-15	3.33	2.0	2.2	2.3	0.0	0.0	1.3	1.1	0.7	1.0
	1-16	4.00	2.0	2.3	2.1	0.0	0.0	1.5	1.0	0.7	1.0
	1- 6	1.33	2.0	2.0	2.1	2.2	—	1.5	1.6	1.6	2.0
	1- 7	1.43	2.0	2.0	2.0	2.2	—	1.4	1.6	1.6	2.0
	1- 8	1.54	1.9	2.0	2.0	2.2	6.9	1.4	1.6	1.5	2.0
	1- 9	1.67	1.9	2.0	2.1	2.2	6.1	1.4	1.5	1.5	2.0
	1-10	1.82	1.9	2.0	2.2	2.2	5.5	1.3	1.5	1.5	2.0
MS2	1-11	2.00	2.0	2.0	2.1	2.2	5.1	1.2	1.4	1.4	2.0
	1-12	2.22	1.8	2.0	2.0	2.2	4.7	1.1	1.4	1.4	2.0
	1-13	2.50	1.7	2.0	2.1	2.2	4.3	1.0	1.3	1.3	2.0
	1-14	2.86	1.7	2.0	2.3	2.2	4.0	0.8	1.2	1.2	2.0
	1-15	3.33	1.8	1.9	2.1	2.3	4.0	0.4	1.0	1.0	2.0
	1-16	4.00	1.5	1.8	2.1	2.4	3.7	0.0	0.7	0.6	2.0
	1- 6	1.33	2.0	2.0	2.1	1.8	1.9	1.9	1.9	1.9	2.0
	1- 7	1.43	2.0	2.0	2.2	1.8	1.9	1.9	1.9	1.9	2.0
	1- 8	1.54	2.0	2.0	2.2	1.7	1.9	1.9	1.9	1.9	2.0
	1- 9	1.67	2.0	2.0	2.2	1.7	1.9	1.9	1.9	1.9	2.0
	1-10	1.82	2.0	2.0	2.2	1.7	1.8	1.9	1.9	1.9	2.0
$MS1_{ms}$	1-11	2.00	2.0	2.0	2.2	1.7	1.8	1.9	1.9	1.9	2.0
	1-12	2.22	2.0	2.0	2.2	1.7	1.8	1.8	1.8	1.8	2.0
	1-13	2.50	2.0	2.0	2.2	1.6	1.8	1.8	1.8	1.8	2.0
	1-14	2.86	2.0	2.0	2.2	1.6	1.8	1.8	1.8	1.8	2.0
	1-15	3.33	2.0	2.0	2.2	1.5	1.8	1.8	1.8	1.8	2.0
	1-16	4.00	2.0	2.0	2.2	1.4	1.7	1.7	1.8	1.8	2.0

Table 5: Observed order of accuracy of $\tilde{\nu}$ at the 8 selected locations of set ST2. Spalart & Allmaras one-equation turbulence model.

	Grids	r_{i1}	P1	P2	P3	P4	P5	P6	P7	P8	L_2
	1- 6	1.33	2.0	2.0	2.1	1.9	2.5	1.5	2.0	1.7	2.9
	1- 7	1.43	2.0	2.0	2.2	1.9	2.6	1.4	2.0	1.7	2.8
	1- 8	1.54	2.0	2.0	2.2	1.9	2.6	1.3	2.0	1.7	2.7
	1- 9	1.67	2.0	2.1	2.2	1.9	2.6	1.2	2.0	1.7	2.6
	1-10	1.82	2.0	2.1	2.2	1.9	2.6	1.0	2.0	1.7	2.5
MS4	1-11	2.00	2.0	2.1	2.2	1.9	2.6	0.8	2.0	1.7	2.4
	1-12	2.22	2.0	2.1	2.2	1.9	2.6	0.3	2.0	1.7	2.3
	1-13	2.50	2.0	2.1	2.3	1.8	2.5	0.0	2.0	1.6	2.3
	1-14	2.86	2.0	2.1	2.3	1.8	2.4	0.0	1.9	1.6	2.2
	1-15	3.33	2.0	2.1	2.3	1.6	2.3	0.0	1.9	1.6	2.1
	1-16	4.00	2.0	2.2	2.3	1.5	2.1	—	1.7	1.5	2.1
	1- 6	1.33	1.7	1.7	2.0	2.0	1.9	1.9	1.9	1.7	1.4
	1- 7	1.43	1.9	1.1	2.0	2.0	1.9	1.9	1.9	1.7	1.4
	1- 8	1.54	1.9	1.6	2.0	2.0	1.9	1.9	1.9	1.7	1.4
	1- 9	1.67	1.7	2.3	2.0	1.9	1.9	1.9	1.9	1.7	1.4
	1-10	1.82	1.8	2.1	2.0	1.9	1.9	1.9	1.9	1.7	1.4
MS2	1-11	2.00	1.8	1.9	2.0	1.9	1.9	1.9	1.9	1.6	1.4
	1-12	2.22	1.7	2.2	2.0	1.9	1.9	1.9	1.8	1.6	1.4
	1-13	2.50	1.7	2.5	2.0	1.9	1.9	1.9	1.8	1.6	1.4
	1-14	2.86	1.8	1.9	1.9	1.9	1.9	1.9	1.8	1.5	1.5
	1-15	3.33	1.6	1.7	1.9	1.9	1.9	1.9	1.8	1.4	1.5
	1-16	4.00	1.7	1.8	1.9	1.9	1.9	1.8	1.8	1.3	1.5
	1- 6	1.33	2.0	2.0	2.0	2.0	1.9	2.3	2.1	2.0	1.5
	1- 7	1.43	2.0	2.0	2.0	2.0	1.9	2.4	2.1	2.0	1.5
	1- 8	1.54	2.0	2.0	2.0	2.0	1.9	2.4	2.1	2.0	1.5
	1- 9	1.67	2.0	2.0	2.0	2.0	1.9	2.4	2.1	2.0	1.5
	1-10	1.82	2.0	2.0	2.0	2.0	1.9	2.4	2.1	2.0	1.5
$MS1_{ms}$	1-11	2.00	2.0	2.0	2.0	2.0	1.9	2.4	2.1	2.0	1.5
	1-12	2.22	2.0	2.0	2.0	2.0	1.9	2.4	2.1	2.0	1.5
	1-13	2.50	2.0	2.0	2.0	2.0	1.9	2.4	2.1	2.1	1.5
	1-14	2.86	2.0	2.0	2.0	2.0	1.9	2.5	2.1	2.1	1.5
	1-15	3.33	2.0	2.0	2.0	2.0	1.9	2.5	2.1	2.1	1.6
	1-16	4.00	2.0	2.0	2.0	1.9	1.9	2.5	2.1	2.1	1.6

Table 6: Observed order of accuracy of the convective terms of the $\tilde{\nu}$ transport equation at the 8 selected locations of set ST1. Spalart & Allmaras one-equation turbulence model.

	Grids	r_{i1}	P1	P2	P3	P4	P5	P6	P7	P8	L_2
	1- 6	1.33	2.0	2.2	2.2	1.3	1.0	1.7	2.0	2.0	2.3
	1- 7	1.43	2.0	2.2	2.2	1.3	0.9	1.7	2.0	2.0	2.3
	1- 8	1.54	2.0	2.2	2.3	1.3	0.7	1.6	2.0	2.0	2.2
	1- 9	1.67	2.0	2.2	2.3	1.4	0.5	1.5	2.0	2.0	2.2
	1-10	1.82	2.0	2.2	2.3	1.4	0.3	1.4	2.0	2.0	2.1
MS4	1-11	2.00	2.0	2.3	2.3	1.5	0.0	1.2	2.0	2.0	2.0
	1-12	2.22	2.0	2.3	2.4	1.6	0.0	0.9	2.0	2.0	2.0
	1-13	2.50	2.0	2.3	2.4	1.6	0.0	0.4	2.0	2.0	1.9
	1-14	2.86	2.0	2.4	2.4	1.1	0.0	0.0	2.0	2.0	1.9
	1-15	3.33	2.0	2.5	2.4	0.0	0.3	0.0	2.1	2.0	1.8
	1-16	4.00	2.0	2.7	2.4	0.0	2.2	—	2.2	2.0	1.7
	1- 6	1.33	1.9	2.0	2.1	2.6	1.6	1.7	1.8	1.8	1.5
	1- 7	1.43	1.9	2.0	2.1	2.6	1.5	1.7	1.8	1.8	1.4
	1- 8	1.54	2.1	2.0	2.1	2.6	1.5	1.7	1.8	1.8	1.4
	1- 9	1.67	1.9	2.0	2.1	2.7	1.5	1.7	1.8	1.8	1.4
	1-10	1.82	1.9	2.0	2.1	2.7	1.4	1.7	1.8	1.8	1.4
MS2	1-11	2.00	2.0	2.0	2.1	2.7	1.4	1.6	1.7	1.7	1.4
	1-12	2.22	1.9	2.0	2.1	2.7	1.3	1.6	1.7	1.7	1.4
	1-13	2.50	1.8	2.0	2.1	2.7	1.2	1.6	1.7	1.7	1.5
	1-14	2.86	2.0	2.0	2.1	2.7	1.1	1.5	1.6	1.6	1.5
	1-15	3.33	1.8	2.0	2.1	2.7	0.8	1.4	1.6	1.6	1.5
	1-16	4.00	1.7	2.0	2.1	2.7	0.4	1.3	1.5	1.5	1.5
	1- 6	1.33	2.0	2.0	2.0	2.0	1.9	2.3	2.1	2.0	1.5
	1- 7	1.43	2.0	2.0	2.0	2.0	1.9	2.4	2.1	2.0	1.5
	1- 8	1.54	2.0	2.0	2.0	2.0	1.9	2.4	2.1	2.0	1.5
	1- 9	1.67	2.0	2.0	2.0	2.0	1.9	2.4	2.1	2.0	1.5
	1-10	1.82	2.0	2.0	2.0	2.0	1.9	2.4	2.1	2.0	1.5
$MS1_{ms}$	1-11	2.00	2.0	2.0	2.0	2.0	1.9	2.4	2.1	2.0	1.5
	1-12	2.22	2.0	2.0	2.0	2.0	1.9	2.4	2.1	2.0	1.5
	1-13	2.50	2.0	2.0	2.0	2.0	1.9	2.4	2.1	2.1	1.5
	1-14	2.86	2.0	2.0	2.0	2.0	1.9	2.5	2.1	2.1	1.5
	1-15	3.33	2.0	2.0	2.0	2.0	1.9	2.5	2.1	2.1	1.6
	1-16	4.00	2.0	2.0	2.0	1.9	1.9	2.5	2.1	2.1	1.6

Table 7: Observed order of accuracy of the diffusion terms of the $\tilde{\nu}$ transport equation at the 8 selected locations of set ST1. Spalart & Allmaras one-equation turbulence model.

	Grids	r_{i1}	P1	P2	P3	P4	P5	P6	P7	P8	L_2
	1- 6	1.33	2.0	2.0	2.1	2.0	2.0	0.7	2.0	2.0	1.1
	1- 7	1.43	2.0	2.0	2.1	2.0	2.0	0.5	2.0	2.0	1.1
	1- 8	1.54	2.0	2.0	2.1	1.9	2.0	0.2	2.0	2.1	1.1
	1- 9	1.67	2.0	2.0	2.1	1.9	2.0	0.0	2.0	2.1	1.1
	1-10	1.82	2.0	2.0	2.2	1.9	2.0	0.0	2.0	2.1	1.1
MS4	1-11	2.00	2.0	2.0	2.2	1.9	2.0	0.0	2.0	2.1	1.1
	1-12	2.22	2.0	2.1	2.2	1.9	2.0	0.0	2.0	2.1	1.1
	1-13	2.50	2.0	2.1	2.2	1.8	2.0	—	2.0	2.1	1.1
	1-14	2.86	2.0	2.1	2.3	1.8	2.0	—	2.0	2.1	1.1
	1-15	3.33	2.0	2.1	2.3	1.8	2.1	7.4	2.0	2.1	1.1
	1-16	4.00	2.0	2.1	2.3	1.8	2.1	5.9	2.0	2.1	1.1
	1- 6	1.33	1.8	2.0	2.0	2.1	2.1	2.1	2.1	2.1	2.0
	1- 7	1.43	1.9	2.0	2.0	2.1	2.1	2.1	2.1	2.1	2.0
	1- 8	1.54	2.1	2.0	2.0	2.1	2.1	2.1	2.1	2.1	2.0
	1- 9	1.67	1.8	2.0	2.0	2.1	2.1	2.1	2.1	2.1	2.0
	1-10	1.82	1.8	2.0	2.0	2.1	2.1	2.1	2.1	2.2	2.0
MS2	1-11	2.00	2.0	2.0	2.0	2.1	2.1	2.2	2.2	2.2	2.0
	1-12	2.22	1.8	2.0	2.0	2.1	2.2	2.2	2.2	2.2	2.0
	1-13	2.50	1.7	2.0	2.0	2.1	2.2	2.2	2.2	2.2	2.0
	1-14	2.86	1.9	2.0	2.1	2.1	2.2	2.2	2.2	2.2	2.0
	1-15	3.33	1.7	2.0	2.1	2.1	2.2	2.2	2.2	2.2	2.0
	1-16	4.00	1.6	2.1	2.1	2.1	2.2	2.2	2.2	2.2	2.0
	1- 6	1.33	2.0	2.0	2.1	1.8	1.9	2.0	2.0	2.0	—
	1- 7	1.43	2.0	2.0	2.1	1.8	1.9	2.0	2.0	2.0	—
	1- 8	1.54	2.0	2.0	2.1	1.8	1.9	2.0	2.0	2.0	—
	1- 9	1.67	2.0	2.0	2.1	1.8	1.9	2.0	2.0	2.0	—
	1-10	1.82	2.0	2.0	2.1	1.8	1.9	1.9	2.0	2.0	—
$MS1_{ms}$	1-11	2.00	2.0	2.0	2.1	1.7	1.9	1.9	2.0	2.0	—
	1-12	2.22	2.0	2.0	2.1	1.7	1.9	1.9	2.0	2.0	—
	1-13	2.50	2.0	2.0	2.1	1.7	1.9	1.9	2.0	2.0	—
	1-14	2.86	2.0	2.0	2.1	1.6	1.9	1.9	1.9	2.0	—
	1-15	3.33	2.0	2.0	2.1	1.6	1.9	1.9	1.9	2.0	—
	1-16	4.00	2.0	2.0	2.1	1.5	1.9	1.9	1.9	1.9	—

Table 8: Observed order of accuracy of the production term of the $\tilde{\nu}$ transport equation at the 8 selected locations of set ST1. Spalart & Allmaras one-equation turbulence model.

	Grids	r_{i1}	P1	P2	P3	P4	P5	P6	P7	P8	L_2
	1- 6	1.33	3.3	3.3	3.8	3.8	2.9	0.7	1.9	2.0	1.4
	1- 7	1.43	3.4	3.4	3.9	3.8	3.0	0.4	1.9	2.0	1.4
	1- 8	1.54	3.4	3.5	4.1	3.9	3.0	0.2	1.9	2.0	1.4
	1- 9	1.67	3.5	3.6	4.2	4.0	3.1	0.0	1.9	2.0	1.4
	1-10	1.82	3.7	3.8	4.4	4.2	3.2	0.0	1.9	2.0	1.4
MS4	1-11	2.00	3.8	3.9	4.6	4.3	3.3	0.0	1.9	2.0	1.4
	1-12	2.22	4.0	4.1	4.8	4.5	3.5	0.0	1.9	2.0	1.4
	1-13	2.50	4.2	4.3	5.1	4.6	3.7	—	1.9	2.0	1.4
	1-14	2.86	4.4	4.6	5.5	4.8	3.9	—	1.8	2.0	1.4
	1-15	3.33	4.6	4.9	5.9	5.0	4.1	7.7	1.8	2.0	1.4
	1-16	4.00	4.9	5.3	6.5	5.0	4.3	6.4	1.7	2.0	1.4
	1- 6	1.33	1.9	2.0	2.0	2.1	2.1	2.1	2.1	2.2	2.0
	1- 7	1.43	1.9	2.0	2.0	2.1	2.1	2.1	2.1	2.2	2.0
	1- 8	1.54	2.1	2.0	2.0	2.1	2.1	2.1	2.1	2.2	2.0
	1- 9	1.67	1.9	2.0	2.0	2.1	2.1	2.2	2.2	2.2	2.0
	1-10	1.82	1.9	2.0	2.0	2.1	2.1	2.2	2.2	2.2	2.0
MS2	1-11	2.00	2.1	2.0	2.0	2.1	2.1	2.2	2.2	2.2	2.0
	1-12	2.22	1.9	2.0	2.0	2.1	2.2	2.2	2.2	2.2	2.0
	1-13	2.50	1.9	2.0	2.0	2.1	2.2	2.2	2.2	2.2	2.0
	1-14	2.86	2.0	2.0	2.0	2.1	2.2	2.2	2.2	2.3	2.0
	1-15	3.33	1.8	2.0	2.0	2.1	2.2	2.2	2.2	2.3	2.0
	1-16	4.00	1.8	2.0	2.1	2.1	2.2	2.2	2.2	2.3	2.0
	1- 6	1.33	2.0	2.0	2.1	1.8	1.9	2.0	2.0	2.0	—
	1- 7	1.43	2.0	2.0	2.1	1.8	1.9	2.0	2.0	2.0	—
	1- 8	1.54	2.0	2.0	2.1	1.8	1.9	2.0	2.0	2.0	—
	1- 9	1.67	2.0	2.0	2.1	1.8	1.9	2.0	2.0	2.0	—
	1-10	1.82	2.0	2.0	2.1	1.8	1.9	2.0	2.0	2.0	—
$MS1_{ms}$	1-11	2.00	2.0	2.0	2.1	1.8	1.9	2.0	2.0	2.0	—
	1-12	2.22	2.0	2.0	2.1	1.8	1.9	1.9	2.0	2.0	—
	1-13	2.50	2.0	2.0	2.1	1.7	1.9	1.9	2.0	2.0	—
	1-14	2.86	2.0	2.0	2.1	1.7	1.9	1.9	2.0	2.0	—
	1-15	3.33	2.0	2.0	2.1	1.7	1.9	1.9	2.0	2.0	—
	1-16	4.00	2.0	2.0	2.1	1.6	1.9	1.9	1.9	2.0	—

Table 9: Observed order of accuracy of the dissipation term of the $\tilde{\nu}$ transport equation at the 8 selected locations of set ST1. Spalart & Allmaras one-equation turbulence model.

	Grids	r_{i1}	P1	P2	P3	P4	P5	P6	P7	P8	L_2
	1- 6	1.33	2.1	2.0	2.0	2.0	1.7	2.0	1.9	2.6	0.8
	1- 7	1.43	2.1	2.0	2.0	2.0	1.6	2.0	1.9	2.6	1.4
	1- 8	1.54	2.1	2.0	1.9	2.0	1.6	2.0	1.9	2.7	1.5
	1- 9	1.67	2.1	2.0	1.9	2.0	1.6	2.0	1.9	2.7	1.3
	1-10	1.82	2.2	2.0	1.9	2.0	1.5	1.9	1.9	2.7	1.1
MS4	1-11	2.00	2.2	2.0	1.9	2.0	1.5	1.9	1.8	2.7	0.9
	1-12	2.22	2.2	2.0	1.9	1.9	1.4	1.9	1.8	2.7	0.8
	1-13	2.50	2.2	2.0	1.9	1.9	1.2	1.9	1.8	2.7	0.7
	1-14	2.86	2.2	2.0	1.9	1.9	1.0	1.9	1.8	2.8	0.7
	1-15	3.33	2.3	2.0	1.9	1.9	0.7	1.9	1.7	2.8	0.7
	1-16	4.00	2.3	2.1	1.9	1.9	0.0	1.9	1.7	2.8	0.8
	1- 6	1.33	2.0	2.0	2.0	2.0	1.9	0.6	2.0	1.8	1.9
	1- 7	1.43	2.0	2.0	2.0	2.0	1.9	0.5	2.0	1.8	2.0
	1- 8	1.54	2.0	2.0	2.0	2.0	1.9	0.3	2.0	1.8	2.0
	1- 9	1.67	2.0	2.0	2.0	2.0	1.9	0.0	2.0	1.8	2.0
	1-10	1.82	2.0	2.0	2.0	2.0	1.9	0.0	2.0	1.8	2.0
MS2	1-11	2.00	2.0	2.0	2.0	2.0	1.9	0.0	2.0	1.8	2.0
	1-12	2.22	2.0	2.0	2.0	2.0	1.9	0.0	2.0	1.8	2.0
	1-13	2.50	2.0	2.0	2.0	2.0	1.9	0.0	2.0	1.8	2.0
	1-14	2.86	2.0	2.0	2.0	2.0	1.9	0.0	2.0	1.7	2.0
	1-15	3.33	2.0	2.0	2.0	2.0	1.9	—	2.0	1.7	2.1
	1-16	4.00	2.1	2.0	2.0	2.0	1.8	6.3	2.0	1.7	2.0
	1- 6	1.33	2.0	2.0	2.0	2.0	0.0	2.0	1.8	0.8	2.0
	1- 7	1.43	2.0	2.0	2.0	2.0	0.0	2.0	1.8	0.7	2.0
	1- 8	1.54	2.0	2.0	2.0	1.9	0.0	2.0	1.8	0.6	2.0
	1- 9	1.67	2.0	2.0	2.0	1.9	0.0	2.0	1.8	0.4	2.0
	1-10	1.82	2.0	2.0	2.0	1.9	0.0	2.0	1.8	0.1	2.0
$MS1_{ms}$	1-11	2.00	2.0	2.0	2.0	1.9	0.0	2.0	1.7	0.0	2.0
	1-12	2.22	2.0	2.0	2.0	1.9	—	2.0	1.7	0.0	2.0
	1-13	2.50	2.0	2.0	2.0	1.9	—	2.0	1.7	0.0	2.0
	1-14	2.86	2.0	2.0	2.0	1.9	7.9	2.0	1.6	0.0	2.0
	1-15	3.33	2.0	2.0	2.0	1.9	6.0	2.0	1.6	—	2.0
	1-16	4.00	2.1	2.0	2.0	1.9	5.0	2.0	1.5	7.5	2.0

Table 10: Observed order of accuracy of ν_t at the 8 selected locations of set Eq. Spalart & Allmaras one-equation turbulence model.

	Grids	r_{i1}	P1	P2	P3	P4	P5	P6	P7	P8	L_2
	1- 6	1.33	3.9	4.0	4.7	4.6	3.2	0.7	2.0	2.0	1.3
	1- 7	1.43	4.0	4.1	4.9	4.8	3.3	0.4	2.0	2.0	1.3
	1- 8	1.54	4.2	4.3	5.1	4.9	3.4	0.2	2.0	2.1	1.3
	1- 9	1.67	4.3	4.5	5.3	5.1	3.5	0.0	2.0	2.1	1.3
	1-10	1.82	4.5	4.7	5.5	5.2	3.7	0.0	2.0	2.1	1.2
MS4	1-11	2.00	4.8	4.9	5.8	5.4	3.8	0.0	2.0	2.1	1.2
	1-12	2.22	5.0	5.2	6.2	5.7	4.0	0.0	2.0	2.1	1.2
	1-13	2.50	5.3	5.5	6.7	5.9	4.2	—	2.0	2.1	1.2
	1-14	2.86	5.7	6.0	7.2	6.0	4.4	—	2.0	2.1	1.2
	1-15	3.33	6.1	6.5	7.8	6.1	4.5	7.6	2.0	2.1	1.1
	1-16	4.00	6.6	7.1	—	5.9	4.4	6.3	2.0	2.1	1.1
	1- 6	1.33	1.8	2.0	2.0	2.1	2.1	2.1	2.1	2.2	2.0
	1- 7	1.43	1.9	2.0	2.0	2.1	2.1	2.1	2.1	2.2	2.0
	1- 8	1.54	2.1	2.0	2.0	2.1	2.1	2.1	2.1	2.2	2.0
	1- 9	1.67	1.8	2.0	2.0	2.1	2.1	2.1	2.1	2.2	2.0
	1-10	1.82	1.8	2.0	2.0	2.1	2.1	2.2	2.2	2.2	2.0
MS2	1-11	2.00	2.0	2.0	2.0	2.1	2.1	2.2	2.2	2.2	2.0
	1-12	2.22	1.8	2.0	2.0	2.1	2.2	2.2	2.2	2.2	2.0
	1-13	2.50	1.7	2.0	2.0	2.1	2.2	2.2	2.2	2.2	2.0
	1-14	2.86	1.9	2.0	2.1	2.1	2.2	2.2	2.2	2.2	2.0
	1-15	3.33	1.7	2.0	2.1	2.1	2.2	2.2	2.2	2.3	2.0
	1-16	4.00	1.6	2.1	2.1	2.1	2.2	2.2	2.2	2.3	2.0
	1- 6	1.33	2.0	2.0	2.1	1.8	1.9	2.0	2.0	2.0	2.0
	1- 7	1.43	2.0	2.0	2.1	1.8	1.9	2.0	2.0	2.0	2.0
	1- 8	1.54	2.0	2.0	2.1	1.8	1.9	2.0	2.0	2.0	2.0
	1- 9	1.67	2.0	2.0	2.1	1.8	1.9	2.0	2.0	2.0	2.0
	1-10	1.82	2.0	2.0	2.1	1.8	1.9	2.0	2.0	2.0	2.0
$MS1_{ms}$	1-11	2.00	2.0	2.0	2.1	1.8	1.9	2.0	2.0	2.0	2.0
	1-12	2.22	2.0	2.0	2.1	1.8	1.9	1.9	2.0	2.0	2.0
	1-13	2.50	2.0	2.0	2.1	1.7	1.9	1.9	2.0	2.0	2.0
	1-14	2.86	2.0	2.0	2.1	1.7	1.9	1.9	2.0	2.0	2.0
	1-15	3.33	2.0	2.0	2.1	1.7	1.9	1.9	2.0	2.0	2.0
	1-16	4.00	2.0	2.0	2.1	1.6	1.9	1.9	1.9	2.0	2.0

Table 11: Observed order of accuracy of ν_t at the 8 selected locations of set ST1. Spalart & Allmaras one-equation turbulence model.

	Grids	r_{i1}	P1	P2	P3	P4	P5	P6	P7	P8	L_2
	1- 6	1.33	8.0	—	—	6.8	1.9	1.6	2.2	1.4	1.2
	1- 7	1.43	8.0	—	—	6.5	1.8	1.7	2.3	1.3	1.2
	1- 8	1.54	8.0	—	—	6.1	1.6	1.7	2.2	1.3	1.2
	1- 9	1.67	8.0	—	—	5.7	1.5	1.8	2.2	1.2	1.2
	1-10	1.82	8.0	—	—	5.2	1.3	1.8	2.2	1.1	1.2
MS4	1-11	2.00	—	—	—	4.7	1.2	1.9	2.2	1.1	1.1
	1-12	2.22	—	—	—	4.1	1.0	1.9	2.2	1.0	1.1
	1-13	2.50	—	—	—	3.5	0.8	2.1	2.1	0.9	1.1
	1-14	2.86	—	—	—	2.8	0.5	2.6	1.9	0.8	1.1
	1-15	3.33	—	—	—	2.1	0.4	3.1	1.7	0.7	1.1
	1-16	4.00	—	—	7.9	1.3	1.9	3.1	1.3	0.5	1.0
	1- 6	1.33	1.4	1.5	2.0	2.2	—	1.5	1.6	1.6	2.0
	1- 7	1.43	1.3	1.5	1.9	2.2	—	1.4	1.6	1.6	2.0
	1- 8	1.54	1.2	1.4	1.8	2.2	6.9	1.4	1.6	1.5	2.0
	1- 9	1.67	1.1	1.3	1.9	2.2	6.1	1.4	1.5	1.5	2.0
	1-10	1.82	1.0	1.3	1.9	2.2	5.5	1.3	1.5	1.5	2.0
MS2	1-11	2.00	0.9	1.2	1.8	2.1	5.1	1.2	1.4	1.4	2.0
	1-12	2.22	0.6	1.0	1.7	2.1	4.7	1.1	1.4	1.4	2.0
	1-13	2.50	0.4	0.8	1.7	2.1	4.2	1.0	1.3	1.3	2.0
	1-14	2.86	0.1	0.6	1.8	2.1	4.0	0.8	1.2	1.2	2.0
	1-15	3.33	0.0	0.2	1.5	2.1	4.0	0.4	1.0	1.0	2.0
	1-16	4.00	0.0	0.0	1.3	2.2	3.6	0.0	0.7	0.6	2.0
	1- 6	1.33	2.0	2.0	2.1	1.8	1.9	1.9	1.9	1.9	2.0
	1- 7	1.43	2.0	2.0	2.2	1.8	1.9	1.9	1.9	1.9	2.0
	1- 8	1.54	2.0	2.0	2.2	1.7	1.9	1.9	1.9	1.9	2.0
	1- 9	1.67	2.0	2.0	2.2	1.7	1.9	1.9	1.9	1.9	2.0
	1-10	1.82	2.0	2.0	2.2	1.7	1.8	1.9	1.9	1.9	2.0
$MS1_{ms}$	1-11	2.00	2.0	2.0	2.2	1.7	1.8	1.9	1.9	1.9	2.0
	1-12	2.22	2.0	2.0	2.2	1.7	1.8	1.8	1.8	1.8	2.0
	1-13	2.50	2.0	2.0	2.2	1.6	1.8	1.8	1.8	1.8	2.0
	1-14	2.86	2.0	2.0	2.2	1.6	1.8	1.8	1.8	1.8	2.0
	1-15	3.33	2.0	2.0	2.2	1.5	1.8	1.8	1.8	1.8	2.0
	1-16	4.00	1.9	2.0	2.2	1.4	1.7	1.7	1.8	1.8	2.0

Table 12: Observed order of accuracy of ν_t at the 8 selected locations of set ST2. Spalart & Allmaras one-equation turbulence model.

A.2 Menter one-equation model

This section presents the values of p as a function of the number of grids selected for the following flow variables:

- Dependent variable of the model, $\tilde{\nu}_t$.
  - Grid set Eq.
  - Grid set ST1.
  - Grid set ST2.
- Convection terms of the $\tilde{\nu}_t$ transport equation.
  - Grid set ST1.
- Diffusion terms of the $\tilde{\nu}_t$ transport equation.
  - Grid set ST1.
- Production terms of the $\tilde{\nu}_t$ transport equation.
  - Grid set ST1.
- Dissipation term of the $\tilde{\nu}_t$ transport equation.
  - Grid set ST1.
- Eddy-viscosity, ν_t.
  - Grid set Eq.
  - Grid set ST1.
  - Grid set ST2.

	Grids	r_{i1}	P1	P2	P3	P4	P5	P6	P7	P8	L_2
	1- 6	1.33	2.0	2.0	1.9	1.9	1.9	1.8	1.3	2.2	2.6
	1- 7	1.43	2.0	2.0	1.9	1.9	1.9	1.8	1.2	2.2	2.4
	1- 8	1.54	2.0	2.0	1.9	1.9	1.9	1.8	1.2	2.2	2.2
	1- 9	1.67	2.0	2.0	1.9	1.9	1.9	1.8	1.1	2.2	2.0
	1-10	1.82	2.0	2.0	1.9	1.9	1.9	1.8	1.0	2.2	1.8
MS4	1-11	2.00	2.0	2.0	1.9	1.9	1.9	1.8	0.9	2.2	1.6
	1-12	2.22	2.0	2.0	1.9	1.9	1.9	1.8	0.7	2.2	1.4
	1-13	2.50	2.0	2.0	1.9	1.9	2.0	1.8	0.4	2.3	1.2
	1-14	2.86	2.0	2.0	1.8	1.9	2.0	1.7	0.0	2.3	1.1
	1-15	3.33	2.0	2.0	1.8	1.9	2.0	1.7	0.0	2.3	1.0
	1-16	4.00	2.0	2.0	1.8	1.8	2.0	1.6	0.0	2.4	0.8
	1- 6	1.33	2.0	2.0	2.0	1.9	1.8	2.3	1.9	1.3	1.9
	1- 7	1.43	2.0	2.0	2.0	1.9	1.8	2.3	1.9	1.3	1.9
	1- 8	1.54	2.0	2.0	2.0	1.9	1.8	2.3	1.9	1.3	1.9
	1- 9	1.67	2.0	2.0	2.0	1.9	1.8	2.3	1.9	1.2	1.9
	1-10	1.82	2.0	2.0	2.0	1.9	1.7	2.3	1.9	1.1	1.9
$MS2_{mp}$	1-11	2.00	2.0	2.0	1.9	1.9	1.7	2.3	1.9	1.0	1.9
	1-12	2.22	2.0	2.0	1.9	1.9	1.7	2.3	1.9	0.8	1.9
	1-13	2.50	2.0	2.0	1.9	1.9	1.7	2.4	1.9	0.6	2.0
	1-14	2.86	2.0	1.9	1.9	1.9	1.6	2.4	1.9	0.3	2.0
	1-15	3.33	2.0	1.9	1.9	1.9	1.6	2.4	2.0	0.0	2.0
	1-16	4.00	2.0	1.9	1.9	1.9	1.4	2.5	2.0	0.0	2.0
	1- 6	1.33	2.0	2.0	1.9	1.9	2.2	1.9	1.1	6.3	2.0
	1- 7	1.43	2.0	2.0	2.0	1.9	2.2	1.9	1.0	5.8	2.0
	1- 8	1.54	2.0	2.0	1.9	1.8	2.2	1.9	0.9	5.4	2.0
	1- 9	1.67	2.0	2.0	2.0	1.8	2.2	1.9	0.8	5.1	2.0
	1-10	1.82	2.0	2.0	1.9	1.8	2.2	1.9	0.6	4.8	2.0
MS1	1-11	2.00	2.0	2.0	1.9	1.8	2.3	1.9	0.4	4.5	2.0
	1-12	2.22	2.0	2.0	1.9	1.8	2.3	1.9	0.1	4.3	2.0
	1-13	2.50	2.0	2.0	1.9	1.8	2.3	1.9	0.0	4.1	2.0
	1-14	2.86	2.0	2.0	1.9	1.8	2.3	1.9	0.0	3.9	2.0
	1-15	3.33	2.0	2.0	1.9	1.7	2.3	1.9	0.0	3.8	2.0
	1-16	4.00	2.0	2.0	1.9	1.6	2.4	2.0	0.0	3.6	2.0

Table 13: Observed order of accuracy of $\tilde{\nu}_t$ at the 8 selected locations of set Eq. Menter one-equation turbulence model.

	Grids	r_{i1}	P1	P2	P3	P4	P5	P6	P7	P8	L_2
	1- 6	1.33	2.0	2.0	2.0	2.0	2.1	2.0	2.0	1.9	1.7
	1- 7	1.43	2.0	2.0	2.0	2.0	2.1	2.0	2.1	1.9	1.8
	1- 8	1.54	2.0	2.0	2.0	2.0	2.1	2.0	2.1	1.9	1.9
	1- 9	1.67	2.0	2.0	2.0	2.0	2.1	2.0	2.1	1.9	2.1
	1-10	1.82	2.0	2.0	2.0	2.0	2.1	2.0	2.1	1.9	2.2
MS4	1-11	2.00	2.0	2.0	2.0	2.1	2.1	2.0	2.1	1.9	2.3
	1-12	2.22	2.0	2.0	2.0	2.1	2.1	2.0	2.1	1.8	2.5
	1-13	2.50	2.0	2.0	2.0	2.1	2.2	2.0	2.1	1.8	2.8
	1-14	2.86	2.0	2.0	2.0	2.1	2.2	2.0	2.1	1.8	3.1
	1-15	3.33	2.0	2.0	1.9	2.1	2.2	2.0	2.1	1.8	3.5
	1-16	4.00	2.0	1.9	1.9	2.2	2.3	1.9	2.1	1.7	3.5
	1- 6	1.33	1.9	2.0	2.0	2.0	2.0	2.0	2.0	2.0	1.9
	1- 7	1.43	1.9	2.0	2.0	2.0	2.0	2.0	2.0	2.0	1.8
	1- 8	1.54	1.9	2.0	2.0	2.0	2.0	2.0	2.0	2.0	1.8
	1- 9	1.67	1.9	2.0	2.0	2.0	2.0	2.0	2.0	2.0	1.8
	1-10	1.82	1.9	2.0	2.0	2.0	2.0	2.0	2.0	2.0	1.8
$MS2_{mp}$	1-11	2.00	1.9	2.0	2.0	2.0	2.0	2.0	2.0	2.0	1.8
	1-12	2.22	1.9	2.0	2.0	2.0	2.0	2.0	2.0	2.0	1.8
	1-13	2.50	1.9	2.0	2.0	2.0	2.0	2.0	2.0	2.0	1.8
	1-14	2.86	1.9	2.0	2.0	2.0	2.0	2.0	2.0	2.0	1.8
	1-15	3.33	1.8	1.9	2.0	2.0	2.0	2.0	2.0	2.0	1.7
	1-16	4.00	1.8	1.9	2.0	2.0	2.0	2.0	2.0	2.0	1.7
	1- 6	1.33	2.0	2.0	2.0	2.0	2.0	2.1	2.1	2.5	2.0
	1- 7	1.43	2.0	2.0	2.0	2.0	2.0	2.1	2.1	2.5	2.0
	1- 8	1.54	2.0	2.0	2.0	2.0	2.0	2.1	2.1	2.5	2.0
	1- 9	1.67	2.0	2.0	2.0	2.0	2.0	2.1	2.1	2.5	2.0
	1-10	1.82	2.0	2.0	2.0	2.0	2.0	2.1	2.1	2.5	2.0
MS1	1-11	2.00	2.0	2.0	2.0	2.0	2.0	2.1	2.1	2.6	2.0
	1-12	2.22	2.0	2.0	2.0	2.0	2.0	2.1	2.1	2.6	2.0
	1-13	2.50	2.0	2.0	2.0	2.0	2.0	2.1	2.1	2.6	2.0
	1-14	2.86	2.0	2.0	2.0	2.0	2.1	2.1	2.2	2.6	2.0
	1-15	3.33	2.0	2.0	2.0	2.0	2.1	2.1	2.2	2.6	2.0
	1-16	4.00	2.0	2.0	2.0	2.0	2.1	2.1	2.2	2.7	2.0

Table 14: Observed order of accuracy of $\tilde{\nu}_t$ at the 8 selected locations of set ST1. Menter one-equation turbulence model.

	Grids	r_{i1}	P1	P2	P3	P4	P5	P6	P7	P8	L_2
	1- 6	1.33	2.0	2.0	1.8	1.1	0.3	0.1	0.4	0.9	2.3
	1- 7	1.43	2.0	2.0	1.8	1.1	0.3	0.2	0.4	1.0	2.4
	1- 8	1.54	2.0	2.0	1.8	1.1	0.3	0.2	0.4	1.1	2.5
	1- 9	1.67	2.0	2.0	1.8	1.0	0.3	0.2	0.5	1.2	2.7
	1-10	1.82	2.0	2.0	1.8	1.0	0.2	0.2	0.5	1.4	2.8
MS4	1-11	2.00	2.0	2.0	1.7	0.9	0.2	0.2	0.6	1.6	3.1
	1-12	2.22	2.0	2.0	1.7	0.9	0.2	0.2	0.7	1.9	3.4
	1-13	2.50	2.0	2.0	1.7	0.8	0.2	0.3	0.8	2.5	3.9
	1-14	2.86	2.0	1.9	1.6	0.8	0.2	0.3	1.1	3.6	4.0
	1-15	3.33	2.0	1.9	1.6	0.7	0.2	0.5	1.7	5.1	3.6
	1-16	4.00	2.0	1.9	1.5	0.6	0.3	0.7	3.9	4.9	2.9
	1- 6	1.33	1.9	1.4	0.7	1.4	1.7	1.8	1.9	1.9	1.6
	1- 7	1.43	1.9	1.3	0.5	1.4	1.7	1.8	1.9	1.9	1.6
	1- 8	1.54	1.9	1.2	0.2	1.3	1.7	1.8	1.9	1.9	1.5
	1- 9	1.67	1.9	1.1	0.0	1.1	1.7	1.8	1.9	1.9	1.5
	1-10	1.82	1.9	0.9	0.0	0.9	1.6	1.8	1.8	1.9	1.5
$MS2_{mp}$	1-11	2.00	1.9	0.6	0.0	0.7	1.6	1.8	1.8	1.9	1.5
	1-12	2.22	1.9	0.2	0.0	0.2	1.6	1.8	1.8	1.9	1.5
	1-13	2.50	1.9	0.0	0.0	0.0	1.5	1.7	1.8	1.9	1.5
	1-14	2.86	1.9	0.0	0.0	0.0	1.3	1.7	1.8	1.9	1.5
	1-15	3.33	1.8	0.0	0.0	0.0	0.8	1.7	1.8	1.9	1.5
	1-16	4.00	1.8	0.0	0.0	0.0	0.3	1.7	1.8	1.9	1.5
	1- 6	1.33	2.0	2.0	2.0	2.0	2.0	2.1	2.1	2.1	2.0
	1- 7	1.43	2.0	2.0	2.0	2.0	2.0	2.1	2.1	2.1	2.0
	1- 8	1.54	2.0	2.0	2.0	2.0	2.1	2.1	2.1	2.1	2.0
	1- 9	1.67	2.0	2.0	2.0	2.0	2.1	2.1	2.1	2.1	2.0
	1-10	1.82	2.0	2.0	2.0	2.0	2.1	2.1	2.1	2.1	2.0
MS1	1-11	2.00	2.0	2.0	2.0	2.0	2.1	2.1	2.1	2.1	2.0
	1-12	2.22	2.0	2.0	2.0	2.0	2.1	2.1	2.1	2.1	2.0
	1-13	2.50	2.0	2.0	2.0	2.0	2.1	2.1	2.1	2.1	2.1
	1-14	2.86	2.0	2.0	2.0	2.0	2.1	2.1	2.1	2.1	2.1
	1-15	3.33	2.1	2.0	2.0	2.1	2.1	2.1	2.1	2.1	2.1
	1-16	4.00	2.1	2.1	2.1	2.1	2.1	2.1	2.1	2.2	2.1

Table 15: Observed order of accuracy of $\tilde{\nu}_t$ at the 8 selected locations of set ST2. Menter one-equation turbulence model.

	Grids	r_{i1}	P1	P2	P3	P4	P5	P6	P7	P8	L_2
	1- 6	1.33	2.0	2.0	1.9	2.0	2.1	2.1	2.2	1.9	2.0
	1- 7	1.43	2.0	2.0	1.9	2.0	2.2	2.1	2.2	1.9	1.9
	1- 8	1.54	2.0	2.0	1.9	2.1	2.2	2.1	2.2	1.9	1.9
	1- 9	1.67	2.0	2.0	1.9	2.1	2.2	2.1	2.2	1.9	1.8
	1-10	1.82	2.0	2.0	1.9	2.1	2.2	2.1	2.2	1.9	1.8
MS4	1-11	2.00	2.0	2.0	1.9	2.1	2.2	2.1	2.2	1.9	1.8
	1-12	2.22	2.0	1.9	1.9	2.1	2.3	2.1	2.3	1.9	1.9
	1-13	2.50	2.0	1.9	1.9	2.1	2.3	2.1	2.3	1.8	2.0
	1-14	2.86	2.0	1.9	1.9	2.1	2.4	2.1	2.3	1.8	2.2
	1-15	3.33	2.0	1.9	1.9	2.2	2.5	2.1	2.3	1.8	2.5
	1-16	4.00	2.0	1.9	1.8	2.3	2.6	2.0	2.4	1.7	2.6
	1- 6	1.33	2.0	2.0	2.0	2.0	1.9	1.9	1.9	1.8	1.4
	1- 7	1.43	2.0	2.0	2.0	2.0	2.0	1.9	1.9	1.7	1.4
	1- 8	1.54	2.0	2.0	2.0	1.9	1.9	1.9	1.9	1.7	1.4
	1- 9	1.67	2.0	2.0	2.0	1.9	1.8	1.9	1.9	1.7	1.4
	1-10	1.82	2.0	2.0	2.0	1.9	1.8	1.9	1.9	1.7	1.4
$MS2_{mp}$	1-11	2.00	2.0	2.0	1.9	1.9	1.7	1.9	1.9	1.7	1.4
	1-12	2.22	2.0	2.0	1.9	1.9	1.7	1.9	1.9	1.6	1.4
	1-13	2.50	2.0	2.0	1.9	1.9	1.7	1.9	1.9	1.6	1.5
	1-14	2.86	2.0	2.0	1.9	1.9	1.6	1.9	1.9	1.5	1.5
	1-15	3.33	1.9	2.0	1.9	1.9	1.6	1.9	1.8	1.5	1.5
	1-16	4.00	1.9	2.0	1.9	1.8	1.6	1.9	1.8	1.3	1.6
	1- 6	1.33	2.0	2.0	1.9	1.9	1.4	2.2	2.1	2.1	1.2
	1- 7	1.43	2.0	2.0	1.9	1.9	1.4	2.2	2.1	2.1	1.2
	1- 8	1.54	2.0	2.0	1.9	1.9	1.4	2.3	2.1	2.1	1.2
	1- 9	1.67	2.0	2.0	1.9	1.9	1.3	2.3	2.1	2.1	1.2
	1-10	1.82	2.0	1.9	1.9	1.9	1.2	2.3	2.1	2.1	1.2
MS1	1-11	2.00	2.0	1.9	1.9	1.9	1.1	2.3	2.1	2.1	1.2
	1-12	2.22	2.0	1.9	1.9	1.8	1.0	2.3	2.1	2.1	1.2
	1-13	2.50	2.0	1.9	1.9	1.8	0.9	2.3	2.2	2.1	1.2
	1-14	2.86	2.0	1.9	1.9	1.8	0.6	2.3	2.2	2.1	1.2
	1-15	3.33	2.0	1.9	1.9	1.8	0.1	2.4	2.2	2.1	1.2
	1-16	4.00	2.1	1.9	1.9	1.7	0.0	2.4	2.2	2.2	1.3

Table 16: Observed order of accuracy of the convective terms of the $\tilde{\nu}_t$ transport equation at the 8 selected locations of set ST1. Menter one-equation turbulence model.

	Grids	r_{i1}	P1	P2	P3	P4	P5	P6	P7	P8	L_2
	1- 6	1.33	2.0	1.9	1.9	2.1	2.1	2.2	1.7	2.0	1.9
	1- 7	1.43	2.0	1.9	1.9	2.1	2.1	2.2	1.7	1.9	1.9
	1- 8	1.54	2.0	1.8	1.9	2.1	2.1	2.2	1.6	1.9	1.8
	1- 9	1.67	2.0	1.8	1.9	2.1	2.1	2.2	1.6	1.9	1.8
	1-10	1.82	2.0	1.8	1.9	2.1	2.1	2.2	1.5	1.9	1.7
MS4	1-11	2.00	2.0	1.8	1.9	2.2	2.1	2.2	1.5	1.9	1.7
	1-12	2.22	2.0	1.7	1.9	2.2	2.1	2.2	1.4	1.9	1.7
	1-13	2.50	2.0	1.7	1.9	2.2	2.1	2.2	1.3	1.9	1.8
	1-14	2.86	2.0	1.6	1.9	2.3	2.1	2.2	1.1	1.8	1.9
	1-15	3.33	2.0	1.6	1.9	2.4	2.0	2.0	0.9	1.7	2.4
	1-16	4.00	2.0	1.4	1.8	2.5	1.8	1.8	0.5	1.6	2.8
	1- 6	1.33	2.0	2.0	2.0	2.0	1.9	1.9	1.9	1.8	1.4
	1- 7	1.43	2.0	2.0	2.0	2.0	2.0	1.9	1.9	1.8	1.4
	1- 8	1.54	2.0	2.0	2.0	1.9	2.0	1.9	1.9	1.7	1.4
	1- 9	1.67	2.0	2.0	2.0	1.9	1.9	1.9	1.9	1.7	1.4
	1-10	1.82	2.0	2.0	2.0	1.9	1.8	1.9	1.9	1.7	1.4
$MS2_{mp}$	1-11	2.00	2.0	2.0	1.9	1.9	1.8	1.9	1.9	1.7	1.5
	1-12	2.22	2.0	2.0	1.9	1.9	1.7	1.9	1.9	1.7	1.5
	1-13	2.50	2.0	2.0	1.9	1.9	1.7	1.9	1.9	1.6	1.5
	1-14	2.86	2.0	2.0	1.9	1.9	1.6	1.9	1.9	1.6	1.5
	1-15	3.33	1.9	2.0	1.9	1.9	1.6	1.9	1.8	1.5	1.6
	1-16	4.00	1.9	2.0	1.9	1.8	1.6	1.9	1.8	1.4	1.6
	1- 6	1.33	2.0	2.0	2.0	2.0	2.0	2.0	2.0	2.0	1.3
	1- 7	1.43	2.0	2.0	2.0	2.0	2.0	2.0	2.0	1.9	1.3
	1- 8	1.54	2.0	2.0	2.0	2.0	2.0	2.0	2.0	1.9	1.3
	1- 9	1.67	2.0	2.0	2.0	2.0	2.0	2.0	2.1	1.9	1.2
	1-10	1.82	2.0	2.0	2.0	2.0	2.0	2.0	2.1	1.9	1.2
MS1	1-11	2.00	2.0	2.0	2.0	2.0	2.0	2.0	2.1	1.9	1.2
	1-12	2.22	2.0	2.0	2.0	2.0	2.0	2.0	2.1	1.9	1.2
	1-13	2.50	2.0	2.0	2.0	2.0	2.0	2.0	2.1	1.9	1.3
	1-14	2.86	2.0	2.0	2.0	2.0	2.0	2.0	2.1	1.9	1.3
	1-15	3.33	2.0	2.0	2.0	2.0	2.0	2.0	2.1	1.9	1.3
	1-16	4.00	2.0	2.0	2.0	2.0	2.0	2.0	2.1	1.9	1.4

Table 17: Observed order of accuracy of the diffusion terms of the $\tilde{\nu}_t$ transport equation at the 8 selected locations of set ST1. Menter one-equation turbulence model.

	Grids	r_{i1}	P1	P2	P3	P4	P5	P6	P7	P8	L_2
	1- 6	1.33	2.0	2.0	1.9	2.0	2.2	2.1	2.0	1.9	2.6
	1- 7	1.43	2.0	2.0	1.9	2.0	2.2	2.1	2.0	1.9	2.7
	1- 8	1.54	2.0	2.0	1.9	2.0	2.3	2.1	2.0	1.9	2.8
	1- 9	1.67	2.0	2.0	1.9	2.0	2.3	2.1	2.1	1.9	2.8
	1-10	1.82	2.0	2.0	1.9	2.0	2.3	2.1	2.1	1.9	2.9
MS4	1-11	2.00	2.0	2.0	1.9	2.0	2.4	2.1	2.1	1.9	3.0
	1-12	2.22	2.0	2.0	1.9	1.9	2.5	2.1	2.1	1.8	3.1
	1-13	2.50	2.0	1.9	1.9	1.9	2.6	2.1	2.1	1.8	3.2
	1-14	2.86	2.0	1.9	1.9	1.9	2.8	2.1	2.1	1.8	3.4
	1-15	3.33	2.0	1.9	1.9	1.9	3.0	2.0	2.1	1.8	3.6
	1-16	4.00	2.0	1.9	1.8	1.9	3.4	1.9	2.1	1.7	3.4
	1- 6	1.33	2.0	2.0	2.0	2.0	2.0	2.0	2.0	2.0	1.9
	1- 7	1.43	2.0	2.0	2.0	2.0	2.0	2.0	2.0	2.0	1.9
	1- 8	1.54	2.0	2.0	2.0	2.0	2.0	2.0	2.0	2.0	1.9
	1- 9	1.67	2.1	2.0	2.0	2.0	2.0	2.0	2.0	2.0	1.9
	1-10	1.82	2.1	2.0	2.0	2.0	2.0	2.0	2.0	2.0	1.9
$MS2_{mp}$	1-11	2.00	2.1	2.0	2.0	2.0	2.0	2.0	2.0	2.0	1.9
	1-12	2.22	2.1	2.0	2.0	2.0	2.0	2.0	2.0	2.0	1.9
	1-13	2.50	2.1	2.0	2.0	2.0	2.0	2.0	2.0	2.0	1.9
	1-14	2.86	2.1	2.0	2.0	2.0	2.0	2.0	2.0	2.0	1.9
	1-15	3.33	2.1	2.0	2.0	2.0	2.0	2.0	2.0	2.0	1.9
	1-16	4.00	2.2	2.0	2.0	2.0	2.0	2.0	2.0	2.0	1.9
	1- 6	1.33	2.0	2.0	2.0	2.0	2.0	2.0	2.1	2.2	2.0
	1- 7	1.43	2.0	2.0	2.0	2.0	2.0	2.1	2.1	2.2	2.0
	1- 8	1.54	2.0	2.0	2.0	2.0	2.0	2.1	2.1	2.2	2.0
	1- 9	1.67	2.0	2.0	2.0	2.0	2.0	2.1	2.1	2.2	2.0
	1-10	1.82	2.0	2.0	2.0	2.0	2.0	2.1	2.1	2.2	2.0
MS1	1-11	2.00	2.0	2.0	2.0	2.0	2.0	2.1	2.1	2.2	2.0
	1-12	2.22	2.0	2.0	2.0	2.0	2.0	2.1	2.1	2.2	2.0
	1-13	2.50	2.0	2.0	2.0	2.0	2.0	2.1	2.1	2.2	2.0
	1-14	2.86	2.0	2.0	2.0	2.0	2.1	2.1	2.1	2.3	2.0
	1-15	3.33	2.0	2.0	2.0	2.0	2.1	2.1	2.1	2.3	2.0
	1-16	4.00	2.0	2.0	2.0	2.0	2.1	2.1	2.2	2.3	2.0

Table 18: Observed order of accuracy of the production term of the $\tilde{\nu}_t$ transport equation at the 8 selected locations of set ST1. Menter one-equation turbulence model.

	Grids	r_{i1}	P1	P2	P3	P4	P5	P6	P7	P8	L_2
	1- 6	1.33	2.4	2.3	2.1	2.1	2.3	2.2	2.1	1.9	2.0
	1- 7	1.43	2.5	2.3	2.1	2.1	2.3	2.2	2.1	1.9	2.0
	1- 8	1.54	2.5	2.3	2.1	2.2	2.3	2.2	2.1	1.9	2.0
	1- 9	1.67	2.5	2.3	2.1	2.2	2.3	2.2	2.1	1.9	2.0
	1-10	1.82	2.6	2.3	2.2	2.2	2.4	2.2	2.1	1.9	2.0
MS4	1-11	2.00	2.6	2.4	2.2	2.2	2.4	2.3	2.1	1.8	2.0
	1-12	2.22	2.7	2.4	2.2	2.3	2.5	2.3	2.1	1.8	2.0
	1-13	2.50	2.8	2.5	2.2	2.3	2.6	2.3	2.2	1.8	2.0
	1-14	2.86	2.9	2.6	2.3	2.4	2.7	2.4	2.2	1.8	2.0
	1-15	3.33	3.0	2.6	2.3	2.5	2.8	2.4	2.2	1.7	2.0
	1-16	4.00	3.1	2.8	2.4	2.7	3.1	2.5	2.3	1.6	2.1
	1- 6	1.33	2.0	2.0	2.0	2.0	2.0	2.0	2.1	2.0	2.0
	1- 7	1.43	2.0	2.0	2.0	2.0	2.0	2.0	2.1	2.0	2.0
	1- 8	1.54	2.0	2.0	2.0	2.0	2.0	2.0	2.1	2.0	2.0
	1- 9	1.67	2.0	2.0	2.0	2.0	2.0	2.0	2.1	2.0	2.0
	1-10	1.82	2.0	2.0	2.0	2.0	2.0	2.0	2.1	2.0	2.0
$MS2_{mp}$	1-11	2.00	2.1	2.0	2.0	2.0	2.0	2.0	2.1	2.0	2.0
	1-12	2.22	2.1	2.0	2.0	2.0	2.0	2.0	2.1	2.0	2.0
	1-13	2.50	2.1	2.0	2.0	2.0	2.0	2.0	2.1	2.0	2.0
	1-14	2.86	2.1	1.9	2.0	2.0	2.0	2.0	2.1	2.0	2.0
	1-15	3.33	2.1	1.9	1.9	2.0	2.0	2.0	2.1	2.0	2.1
	1-16	4.00	2.1	1.9	1.9	2.0	2.0	2.0	2.1	1.9	2.0
	1- 6	1.33	2.0	2.0	2.0	2.1	2.0	2.0	2.0	2.0	2.1
	1- 7	1.43	2.0	2.0	2.0	2.1	2.0	2.0	2.0	2.0	2.1
	1- 8	1.54	2.0	2.0	2.0	2.1	2.0	2.0	2.0	2.0	2.1
	1- 9	1.67	2.0	2.0	2.0	2.1	1.9	2.0	2.0	2.0	2.1
	1-10	1.82	2.0	2.0	2.0	2.1	1.9	2.0	2.0	2.0	2.1
MS1	1-11	2.00	2.0	2.0	2.0	2.1	1.9	2.0	2.0	2.0	2.1
	1-12	2.22	2.0	2.0	2.0	2.1	1.9	2.0	2.0	2.0	2.1
	1-13	2.50	2.0	2.0	2.0	2.1	1.9	2.0	2.0	2.0	2.1
	1-14	2.86	2.0	2.0	2.0	2.1	1.9	2.0	2.0	2.0	2.1
	1-15	3.33	2.0	2.0	2.0	2.1	1.9	2.0	2.0	2.0	2.1
	1-16	4.00	2.0	2.0	2.0	2.1	1.9	2.0	2.0	2.0	2.1

Table 19: Observed order of accuracy of the dissipation term of the $\tilde{\nu}_t$ transport equation at the 8 selected locations of set ST1. Menter one-equation turbulence model.

	Grids	r_{i1}	P1	P2	P3	P4	P5	P6	P7	P8	L_2
	1- 6	1.33	2.0	2.0	1.9	1.9	1.9	1.8	1.3	2.2	2.1
	1- 7	1.43	2.0	2.0	1.9	1.9	1.9	1.8	1.2	2.2	2.0
	1- 8	1.54	2.0	2.0	1.9	1.9	1.9	1.8	1.2	2.2	1.9
	1- 9	1.67	2.0	2.0	1.9	1.9	1.9	1.8	1.1	2.2	1.7
	1-10	1.82	2.0	2.0	1.9	1.9	1.9	1.8	1.0	2.2	1.6
MS4	1-11	2.00	2.0	2.0	1.9	1.9	1.9	1.8	0.9	2.2	1.4
	1-12	2.22	2.0	2.0	1.9	1.9	1.9	1.8	0.7	2.2	1.3
	1-13	2.50	2.0	2.0	1.9	1.9	2.0	1.8	0.4	2.3	1.2
	1-14	2.86	2.0	2.0	1.8	1.9	2.0	1.7	0.0	2.3	1.0
	1-15	3.33	2.0	2.0	1.8	1.9	2.0	1.7	0.0	2.3	1.0
	1-16	4.00	2.0	2.0	1.8	1.8	2.0	1.6	0.0	2.4	0.8
	1- 6	1.33	2.0	2.0	2.0	1.9	1.8	2.3	1.9	1.3	2.2
	1- 7	1.43	2.0	2.0	2.0	1.9	1.8	2.3	1.9	1.3	2.4
	1- 8	1.54	2.0	2.0	2.0	1.9	1.8	2.3	1.9	1.3	2.4
	1- 9	1.67	2.0	2.0	2.0	1.9	1.8	2.3	1.9	1.2	2.3
	1-10	1.82	2.0	2.0	2.0	1.9	1.7	2.3	1.9	1.1	2.1
$MS2_{mp}$	1-11	2.00	2.0	2.0	1.9	1.9	1.7	2.3	1.9	1.0	1.9
	1-12	2.22	2.0	2.0	1.9	1.9	1.7	2.3	1.9	0.8	1.7
	1-13	2.50	2.0	2.0	1.9	1.9	1.7	2.4	1.9	0.6	1.6
	1-14	2.86	2.0	1.9	1.9	1.9	1.6	2.4	1.9	0.3	1.7
	1-15	3.33	2.0	1.9	1.9	1.9	1.6	2.4	2.0	0.0	1.9
	1-16	4.00	2.0	1.9	1.9	1.9	1.4	2.5	2.0	0.0	2.1
	1- 6	1.33	2.0	2.0	1.9	1.9	2.2	1.9	1.1	6.3	2.0
	1- 7	1.43	2.0	2.0	2.0	1.9	2.2	1.9	1.0	5.8	2.0
	1- 8	1.54	2.0	2.0	1.9	1.8	2.2	1.9	0.9	5.4	2.0
	1- 9	1.67	2.0	2.0	2.0	1.8	2.2	1.9	0.8	5.1	2.0
	1-10	1.82	2.0	2.0	1.9	1.8	2.2	1.9	0.6	4.8	2.0
MS1	1-11	2.00	2.0	2.0	1.9	1.8	2.3	1.9	0.4	4.5	2.0
	1-12	2.22	2.0	2.0	1.9	1.8	2.3	1.9	0.1	4.3	2.0
	1-13	2.50	2.0	2.0	1.9	1.8	2.3	1.9	0.0	4.1	2.0
	1-14	2.86	2.0	2.0	1.9	1.8	2.3	1.9	0.0	3.9	2.0
	1-15	3.33	2.0	2.0	1.9	1.7	2.3	1.9	0.0	3.8	2.0
	1-16	4.00	2.0	2.0	1.9	1.6	2.4	2.0	0.0	3.6	2.0

Table 20: Observed order of accuracy of ν_t at the 8 selected locations of set Eq. Menter one-equation turbulence model.

	Grids	r_{i1}	P1	P2	P3	P4	P5	P6	P7	P8	L_2
	1- 6	1.33	2.9	2.5	2.2	2.2	2.4	2.1	2.0	1.9	2.4
	1- 7	1.43	2.9	2.6	2.3	2.3	2.4	2.1	2.0	1.9	2.4
	1- 8	1.54	3.0	2.6	2.3	2.3	2.5	2.1	2.0	1.9	2.5
	1- 9	1.67	3.1	2.7	2.3	2.3	2.5	2.1	2.1	1.9	2.5
	1-10	1.82	3.2	2.7	2.3	2.4	2.6	2.1	2.1	1.9	2.6
MS4	1-11	2.00	3.3	2.8	2.4	2.4	2.6	2.1	2.1	1.9	2.7
	1-12	2.22	3.4	2.9	2.4	2.5	2.7	2.1	2.1	1.8	2.8
	1-13	2.50	3.6	3.0	2.5	2.5	2.9	2.1	2.1	1.8	2.9
	1-14	2.86	3.8	3.2	2.6	2.7	3.0	2.1	2.1	1.8	3.1
	1-15	3.33	4.1	3.4	2.7	2.9	3.3	2.0	2.1	1.8	3.4
	1-16	4.00	4.4	3.7	2.9	3.2	3.6	1.9	2.1	1.7	3.3
	1- 6	1.33	2.1	2.0	2.0	2.0	2.0	2.0	2.0	2.0	1.9
	1- 7	1.43	2.1	2.0	2.0	2.0	2.0	2.0	2.0	2.0	1.9
	1- 8	1.54	2.1	2.0	2.0	2.0	2.0	2.0	2.0	2.0	1.9
	1- 9	1.67	2.1	2.0	2.0	2.0	2.0	2.0	2.0	2.0	1.9
	1-10	1.82	2.1	2.0	2.0	2.0	2.0	2.0	2.0	2.0	1.9
$MS2_{mp}$	1-11	2.00	2.2	2.0	2.0	2.0	2.0	2.0	2.0	2.0	1.9
	1-12	2.22	2.2	2.0	2.0	2.0	2.0	2.0	2.0	2.0	1.9
	1-13	2.50	2.2	2.0	2.0	2.0	2.0	2.0	2.0	2.0	1.9
	1-14	2.86	2.2	2.0	2.0	2.0	2.0	2.0	2.0	2.0	1.9
	1-15	3.33	2.3	2.0	2.0	2.0	2.0	2.0	2.0	2.0	1.9
	1-16	4.00	2.3	2.0	2.0	2.0	2.0	2.0	2.0	2.0	1.9
	1- 6	1.33	2.0	2.0	2.0	2.0	2.0	2.1	2.1	2.5	2.0
	1- 7	1.43	2.0	2.0	2.0	2.0	2.0	2.1	2.1	2.5	2.0
	1- 8	1.54	2.0	2.0	2.0	2.0	2.0	2.1	2.1	2.5	2.0
	1- 9	1.67	2.0	2.0	2.0	2.0	2.0	2.1	2.1	2.5	2.0
	1-10	1.82	2.0	2.0	2.0	2.0	2.0	2.1	2.1	2.5	2.0
MS1	1-11	2.00	2.0	2.0	2.0	2.0	2.0	2.1	2.1	2.6	2.0
	1-12	2.22	2.0	2.0	2.0	2.0	2.0	2.1	2.1	2.6	2.0
	1-13	2.50	2.0	2.0	2.0	2.0	2.0	2.1	2.1	2.6	2.0
	1-14	2.86	2.0	2.0	2.0	2.0	2.1	2.1	2.2	2.6	2.0
	1-15	3.33	2.0	2.0	2.0	2.0	2.1	2.1	2.2	2.6	2.0
	1-16	4.00	2.0	2.0	2.0	2.0	2.1	2.1	2.2	2.7	2.0

Table 21: Observed order of accuracy of ν_t at the 8 selected locations of set ST1. Menter one-equation turbulence model.

	Grids	r_{i1}	P1	P2	P3	P4	P5	P6	P7	P8	L_2
	1- 6	1.33	6.0	5.9	5.6	4.2	2.1	1.3	1.4	2.2	2.7
	1- 7	1.43	6.0	5.9	5.6	4.1	2.1	1.3	1.4	2.3	2.7
	1- 8	1.54	6.0	5.9	5.6	4.0	2.0	1.3	1.4	2.4	2.8
	1- 9	1.67	6.0	5.9	5.5	3.9	1.9	1.3	1.5	2.6	2.9
	1-10	1.82	6.0	5.9	5.5	3.7	1.9	1.3	1.5	2.8	3.0
MS4	1-11	2.00	6.0	5.9	5.4	3.6	1.8	1.3	1.6	3.1	3.1
	1-12	2.22	6.0	5.9	5.3	3.4	1.7	1.3	1.7	3.7	3.3
	1-13	2.50	5.9	5.9	5.2	3.2	1.7	1.3	1.9	4.8	3.6
	1-14	2.86	5.9	5.8	5.1	3.0	1.6	1.4	2.4	7.1	3.7
	1-15	3.33	5.9	5.8	4.8	2.8	1.6	1.5	3.5	—	3.3
	1-16	4.00	5.9	5.7	4.6	2.6	1.6	2.0	—	5.4	2.7
	1- 6	1.33	4.2	0.0	0.0	0.0	0.8	1.6	1.9	1.9	1.8
	1- 7	1.43	4.3	0.0	0.0	0.0	0.7	1.6	1.9	1.9	1.8
	1- 8	1.54	4.4	0.0	0.0	0.0	0.6	1.6	1.9	1.9	1.8
	1- 9	1.67	4.5	0.0	0.0	0.0	0.5	1.5	1.9	1.9	1.8
	1-10	1.82	4.6	0.0	0.0	0.0	0.3	1.5	1.9	1.9	1.8
$MS2_{mp}$	1-11	2.00	4.7	0.0	0.0	0.0	0.1	1.4	1.9	1.9	1.8
	1-12	2.22	4.8	0.0	0.0	0.0	0.0	1.3	1.9	1.9	1.8
	1-13	2.50	4.8	0.0	0.0	0.0	0.0	1.2	1.9	1.9	1.8
	1-14	2.86	4.9	0.0	0.0	0.0	0.0	1.1	1.9	1.9	1.8
	1-15	3.33	5.0	0.0	0.0	0.0	0.0	0.9	1.9	1.9	1.7
	1-16	4.00	5.0	0.0	0.0	0.0	0.0	0.6	1.9	1.9	1.7
	1- 6	1.33	2.0	2.0	2.0	2.0	2.0	2.1	2.1	2.1	2.0
	1- 7	1.43	2.0	2.0	2.0	2.0	2.0	2.1	2.1	2.1	2.0
	1- 8	1.54	2.0	2.0	2.0	2.0	2.1	2.1	2.1	2.1	2.0
	1- 9	1.67	2.0	2.0	2.0	2.0	2.1	2.1	2.1	2.1	2.0
	1-10	1.82	2.0	2.0	2.0	2.0	2.1	2.1	2.1	2.1	2.0
MS1	1-11	2.00	2.0	2.0	2.0	2.0	2.1	2.1	2.1	2.1	2.0
	1-12	2.22	2.0	2.0	2.0	2.0	2.1	2.1	2.1	2.1	2.0
	1-13	2.50	2.0	2.0	2.0	2.0	2.1	2.1	2.1	2.1	2.1
	1-14	2.86	2.0	2.0	2.0	2.0	2.1	2.1	2.1	2.1	2.1
	1-15	3.33	2.1	2.0	2.0	2.1	2.1	2.1	2.1	2.1	2.1
	1-16	4.00	2.1	2.1	2.1	2.1	2.1	2.1	2.1	2.2	2.1

Table 22: Observed order of accuracy of ν_t at the 8 selected locations of set ST2. Menter one-equation turbulence model.

B Fortran Functions

As for the original MS, [1], all the functions have been written in FORTRAN 90 with double precision (REAL*8) variables. The structure of the functions is identical for the MS2 and MS2P. The input arguments of all the functions are the Cartesian coordinates x and y. The argument of the damping functions of the one-equation models is the dependent variable of the model, $\tilde{\nu}$.

B.1 Main flow variables

B.1.1 u velocity component

Name	Arguments	Output
UMS	x, y	Horizontal velocity component, u
DUDXMS	x, y	Derivative of u with respect to x, $\frac{\partial u}{\partial x}$
DUDYMS	x, y	Derivative of u with respect to y, $\frac{\partial u}{\partial y}$
DUDX2MS	x, y	Second derivative of u with respect to x, $\frac{\partial^2 u}{\partial x^2}$
DUDY2MS	x, y	Second derivative of u with respect to y, $\frac{\partial^2 u}{\partial y^2}$
DUDXYMS	x, y	Second-order cross-derivative of u, $\frac{\partial^2 u}{\partial x \partial y}$

B.1.2 v velocity component

Name	Arguments	Output
VMS	x, y	Vertical velocity component, v
DVDXMS	x, y	Derivative of v with respect to x, $\frac{\partial v}{\partial x}$
DVDYMS	x, y	Derivative of v with respect to y, $\frac{\partial v}{\partial y}$
DVDX2MS	x, y	Second derivative of v with respect to x, $\frac{\partial^2 v}{\partial x^2}$
DVDY2MS	x, y	Second derivative of v with respect to y, $\frac{\partial^2 v}{\partial y^2}$
DVDXYMS	x, y	Second-order cross-derivative of v, $\frac{\partial^2 v}{\partial x \partial y}$

B.1.3 Pressure, C_p

Name	Arguments	Output
PMS	x, y	Pressure coefficient, $C_p = \frac{p-p_{ref}}{\rho U_{ref}^2}$
DPDXMS	x, y	Derivative of C_p with respect to x, $\frac{\partial C_p}{\partial x}$
DPDYMS	x, y	Derivative of C_p with respect to y, $\frac{\partial C_p}{\partial y}$

B.1.4 Eddy-Viscosity, ν_t

- One-equation turbulence model
  - Spalart & Allmaras

Name	Arguments	Output
EDDYSAMS	x, y	Eddy-Viscosity, ν_t
DESADXMS	x, y	Derivative of ν_t with respect to x, $\frac{\partial \nu_t}{\partial x}$
DESADYMS	x, y	Derivative of ν_t with respect to y, $\frac{\partial \nu_t}{\partial y}$

  - Menter

Name	Arguments	Output
EDDYMTMS	x, y	Eddy-Viscosity, ν_t
DEMTDXMS	x, y	Derivative of ν_t with respect to x, $\frac{\partial \nu_t}{\partial x}$
DEMTDYMS	x, y	Derivative of ν_t with respect to y, $\frac{\partial \nu_t}{\partial y}$

B.1.5 Auxiliary variables

Name	Arg.	Output
VORTMS	x, y	Magnitude of Vorticity, $S_\Omega = \left\lvert \frac{\partial u}{\partial y} - \frac{\partial v}{\partial x} \right\rvert$
STRAINMS	x, y	Strain-rate, $\sqrt{S} = \sqrt{2\left(\left(\frac{\partial u}{\partial x}\right)^2 + \left(\frac{\partial v}{\partial y}\right)^2\right) + \left(\frac{\partial u}{\partial y} + \frac{\partial v}{\partial x}\right)^2}$

B.2 Source terms of the momentum equations

B.2.1 One-equation turbulence models

- Spalart & Allmaras

Name	Arguments	Output
SMXSAMS	x, y	Source function of the x momentum equation, f_x
SMYSAMS	x, y	Source function of the y momentum equation, f_y

- Menter

Name	Arguments	Output
SMXMTMS	x, y	Source function of the x momentum equation, f_x
SMYMTMS	x, y	Source function of the y momentum equation, f_y

B.3 One-equation Turbulence models

B.3.1 Spalart & Allmaras

Name	Arguments	Output
SSAMS	x, y	Source function of the $\tilde{\nu}$ transport equation, f_{spal}
EM1MS	x, y	Dependent variable of the turbulence model, $\tilde{\nu}$
DEM1DXMS	x, y	Derivative of $\tilde{\nu}$ with respect to x, $\frac{\partial \tilde{\nu}}{\partial x}$
DEM1DYMS	x, y	Derivative of $\tilde{\nu}$ with respect to y, $\frac{\partial \tilde{\nu}}{\partial y}$
DEM1DX2MS	x, y	Second derivative of $\tilde{\nu}$ with respect to x, $\frac{\partial^2 \tilde{\nu}}{\partial x^2}$
DEM1DY2MS	x, y	Second derivative of $\tilde{\nu}$ with respect to y, $\frac{\partial^2 \tilde{\nu}}{\partial y^2}$
FV1SAMS	$\tilde{\nu}$	Damping function of the model
DFV1SAMS	$\tilde{\nu}$	Derivative of the damping function with respect to $\tilde{\nu}$

B.3.2 Menter

Name	Arguments	Output
SMTMS	x, y	Source function of the $\tilde{\nu}_t$ transport equation, f_{mnt}
EM1MS	x, y	Dependent variable of the turbulence model, $\tilde{\nu}_t$
DEM1DXMS	x, y	Derivative of $\tilde{\nu}_t$ with respect to x, $\frac{\partial \tilde{\nu}_t}{\partial x}$
DEM1DYMS	x, y	Derivative of $\tilde{\nu}_t$ with respect to y, $\frac{\partial \tilde{\nu}_t}{\partial y}$
DEM1DX2MS	x, y	Second derivative of $\tilde{\nu}_t$ with respect to x, $\frac{\partial^2 \tilde{\nu}_t}{\partial x^2}$
DEM1DY2MS	x, y	Second derivative of $\tilde{\nu}_t$ with respect to y, $\frac{\partial^2 \tilde{\nu}_t}{\partial y^2}$
D2MTMS	$\tilde{\nu}_t$	Damping function of the model
DD2MTMS	$\tilde{\nu}_t$	Derivative of the damping function with respect to $\tilde{\nu}_t$